UNIVERSITY OF PADOVA

Department of

LAND, ENVIRONMENT, AGRICULTURE AND FORESTRY

Master's degree in

Forest Science – forest and land management

Interaction between channel control works and sediment dynamics: a multi-temporal approach

Supervisor:
Prof. Dr. Lorenzo Picco

Co-supervisor:
Dr. Lorenzo Martini

Graduating student:
Francesco Piccinin
Matriculation n. 2024267

ACADEMIC YEAR 2021-2022

Abstract

La gestione dell'erosione e del trasporto di sedimento nei torrenti montani viene effettuato attraverso la costruzione di sistemazioni idrauliche all'interno del canale. Tra le diverse tipologie, le briglie sono le strutture più comuni e diffuse per gestire i flussi di sedimento durante gli eventi di piena. La progettazione delle briglie è basata sul loro ruolo di stabilizzare efficientemente il canale ritenendo il sedimento e prevenendo un'eccessiva erosione che destabilizzerebbe i versanti circostanti. Tuttavia, le opere idrauliche nei torrenti montani hanno un impatto non trascurabile sulle dinamiche di congiunzione del sedimento tra versante e canale e il suo trasferimento lungo quest'ultimo. Quindi, la valutazione degli impatti delle briglie sulle dinamiche del sedimento nei torrenti montani risulta di grande importanza per la manutenzione delle sistemazioni esistenti e per la progettazione di ulteriori opere. Negli ultimi vent'anni, l'evoluzione del paesaggio è stata sempre più studiata tramite dati topografici e con la realizzazione di Modelli Topografici Digitali (DTM) e di Differenze tra DTM (DoD). Nei torrenti montani, il rilevamento dei cambiamenti morfologici attraverso dati topografici multi-temporali permette di comprendere le dinamiche dei processi di erosione e di deposizione e ne permette l'analisi quantitativa.

Lo scopo principale di questa tesi è quello di definire gli effetti di un sistema di briglie sulle dinamiche del sedimento in un canale ripido colpito da un'alluvione improvvisa. L'area di studio è il bacino del torrente Vegliato (UD), avente una superficie di 5 km^2 e caratterizzato dalla presenza di diverse briglie. Per raggiungere questo obiettivo, due DTM, uno dell'anno 2019 e uno del 2022, derivanti da dati LiDAR (Light Detection and Ranging) sono stati utilizzati per creare dei DoD per rilevare e quantificare i processi di erosione e deposizione avvenuti durante la piena improvvisa del 2021 nel torrente Vegliato. L'approccio multi-temporale per il rilevamento dei disegni di erosione e deposizione permette di valutare l'impatto delle briglie sulla ritenzione del sedimento e sui suddetti processi geomorfologici. Le condizioni strutturali e funzionali delle opere sono state anche valutate grazie a rilievi di campo permettendo, quindi, di consolidare i risultati ottenuti con l'analisi dei DoD, dando un'ulteriore visione dettagliata della situazione corrente delle sistemazioni. In prima istanza, i rilievi di campo riportano come la maggior parte delle opere risulti in uno stato di distruzione o di pesante danneggiamento con funzionalità nulla o compromessa. Inoltre, dal momento che alcune briglie risultano ancora in buone condizioni ma presentano uno stato di sovralluvionamento, l'efficienza netta dell'intero sistema, la quale combina stato e funzionalità delle opere, è stimata tra il 25 – 30%. Dall'analisi del DoD è emersa una forte variabilità nei volumi di sedimento, con il canale profondamente colpito da flussi sedimentari e principalmente trasportati durante l'alluvione improvvisa nel periodo studiato. Delle macchie di profonda erosione sono visibili specialmente nella parte superiore del bacino con variazioni verticali nell'ordine di più metri. D'altro canto, le aree di

deposizione sono per lo più presenti nella parte mediana e inferiore dell'area di studio e in corrispondenza di alcuni punti di deviazione del canale dove alcune briglie risultano aggirate.

I risultati di questa ricerca riflettono l'importanza di un monitoraggio costante del sistema fluviale e delle loro opere di sistemazione. In più, ciò che è emerso è l'importanza del ruolo che svolgono i dati topografici multi-temporali, i quali permettono di ottenere un rilevamento dettagliato dei cambiamenti morfologici. Infine, l'uso combinato di dati da telerilevamento e dati ottenuti con rilievi in campo permettono un'appropriata manutenzione delle opere esistenti, specialmente considerando la necessità di ridurre i rischi per la cittadinanza e le attività umane.

Abstract

The management of erosion and sediment transport in mountain streams is performed through the construction of control works within the channel network. Among other typologies, check dams are the most common and widespread hydraulic structures to manage sediment fluxes during flood events. The design of the check dams is based on their role to effectively stabilize the channel retaining sediment and preventing an excess of erosion that might destabilize the surrounding hillslopes. However, channel control works in mountain streams have a non-negligible impact on the coupling dynamics of hillslope-channel sediments and their transfer along the channel. Therefore, the assessment of the impacts of check dams on sediment dynamics in mountain streams is of major importance for the maintenance of the existing control structures and for the designing of new ones. In the last twenty years, the evolution of landscape has increasingly been studied through topographical data and with the realization of Digital Terrain Models (DTMs) and DTMs of Difference (DoDs). In mountain streams, the detection of morphological changes through multi-temporal topographical data helps the understanding of the dynamics of erosion and deposition patterns and allows their quantitative analysis.

The main aim of this thesis is to define the effects of check dams on sediment dynamics in a steep channel affected by a flash flood. The study area is the Vegliato Torrent basin (UD), a 5 km^2 catchment characterized by the presence of several check dams. To achieve the objective, multi-temporal DTMs derived from Light Detection and Ranging (LiDAR) data for 2019 and 2022 are used to create DoDs to detect and quantify erosion and deposition processes occurred during the 2021 flash flood event in Vegliato Torrent. The multi-temporal approach for the detection of erosion and deposition patterns allows to assess the impact of the check dams on sediment retention and on erosion and deposition processes. The structural and functional conditions of the channel works were also evaluated thanks to field surveys, hence supporting the findings of the DoD analysis and giving a more detailed view of the current situation of the channel control system. First, the field surveys show

that the majority of the check dams are in a destroyed or heavily damaged state with ceased or compromised functionality. Moreover, since some check dams are in good structural conditions but present a sediment over-flooded state, the overall system's net efficiency, which combines state and functionality, is estimated in the range of 25-30%. . From the DoDs analysis, a strong variability in sediment volumes emerged, with the channel network deeply affected by sediment fluxes during the study period and mainly conveyed during the flash flood. Patches of deep erosion are visible especially in the upper part of the basin with vertical variations in the order of meters. On the other hand, deposition areas are present in the middle-lower section of the study area and in correspondence of some points of stream's diversion where some check dams are outflanked.

The results of this research reflect the importance of the constant monitoring of the fluvial system and the channel control works. Moreover, what has emerged is the importance of high resolution and multi-temporal data, thanks to which is possible to achieve a detailed detection of morphological changes. Finally, the combined use of remote sensing data and field surveys will help a proper maintenance of the existent works, especially considering the need to reduce risks for human settlements and activities.

Table of contents

1. Introduction

The magnitude and the timing of floods are affected by the global warming of climate as reported by Bloschl *et al.* (2017), who assessed the changes in the timing of river floods due to climate change in the last 50 years throughout Europe. These changes in climate are observed to impact the temporal occurrence of floods in the European continent from Northeastern Europe to some regions of the Mediterranean coast. Regarding the last one, in the northern coast of the Adriatic Sea, the temporal shift in the flood patterns closely reflect the occurrence of extreme precipitations (Bloschl *et al.*, 2017). In fact, the increase of high-intensity precipitation both at regional and global scale is related to the intensification of the global hydrological cycle resulting from the increase of the water vapor content and energy in the atmosphere due to global warming (Beniston, 2009, Giorgi *et al.*, 2011). Among different types of floods, flash floods are considered the deadliest (Doocy *et al*., 2013) and can result in dangerous and costly outcomes for human lives and activities, (Wilhelm *et al.*, 2012; Esposito *et al.*, 2018; Rainato *et al.*, 2021). Flash floods are defined as abrupt hydrological events characterized by high peak discharges that can heavily impact the geomorphological aspects of fluvial systems in mountain basins (Lucìa *et al.*, 2018). In fact, among several drivers, the main factors triggering these phenomena in mountain watersheds are high intensity thunderstorms and intense precipitation events registered in a limited areal extent, connected to complex interactions of precipitation and soil characteristics (i.e., soil moisture, infiltration capacity) (Bloschl *et al.*, 2017; Shakti *et al*, 2017; Lucìa *et al.*, 2018; Rainato *et al.*, 2021). Gaume *et al*. (2009) set general thresholds in terms of rainfall accumulation, rainfall event duration and areal extent of occurrence to classify flash floods events. Generally, storms that induce flash floods are characterized by a rainfall accumulation that exceeds 100 mm in a very short duration (i.e., less than 24 hours), affecting a limited area of less than 500 km^2. The high intensity of the rainfall events results in a sudden increase of the discharge into the channel network. The responses of the fluvial system to these events include, on the one hand, slope instabilities such as landslides, debris flows and erosion processes, especially in the upstream section of the catchment (Pellegrini *et al.*, 2021). On the other, morphological changes in the channel (i.e., bedform alteration, channel widening and deposition) are frequently observed in the downstream part (Baker, 1977; Pellegrini *et al.*, 2021; Rainato *et al.*, 2021). Furthermore, the impacts of flash floods on sediment dynamics of mountain basins can induce the remobilization of the streambed and the mobilization of boulders along the fluvial system (Turowski *et al.*, 2009; Piton and Recking, 2017). Therefore, during a flash flood, the coupling of the processes occurring in the hillslopes and into the channel can lead to the supply and transport of massive sediment volumes (Baewert and Morche, 2014; Lucìa *et al.*, 2018). Despite of their characteristics that make flash floods one of the most serious natural hazards, these events are still not completely understood and

documented (Gaume *et al*., 2009). Borga *et al.* (2014) report critical issues in monitoring and managing flash flood events, mainly due to their rapid occurrence and the limited temporal gap between the rainfall event and the flood and sediment response. Moreover, the risk for downstream communities is complex to be quantified because of its connection to hydrogeomorphic processes in upstream basins. Therefore, the risk management of these events requires an integrated approach based on effective physical flood protection systems (i.e., control works), the monitoring and management of hillslope processes, geomorphic and hydrological fluvial processes, and the development of strategies for disaster response in a timely manner. The implications for risk management are also reported in detail by Marchi *et al.* (2010). For instance, given the peculiar characteristics of these events, the investigation of these events would require systematic field surveys and ad-hoc analysis after each occurrence. For this reasons, new management strategies based on updated data should be continuously developed. Furthermore, the occurrence of flash floods is related to the seasonality of the rain events, which are strictly connected to climate forcing that need to be considered. Moreover, the geomorphological features of mountain catchments play an important role in anchoring convections and increasing precipitations. This process is combined to the rapid concentration of streamflow due to topographic relief. Eventually, the potential effects of land use change and soil characteristics (i.e., infiltration capacity of the soil and runoff coefficient) are worth to be taken into account since in a disturbed small-size catchment the extreme runoff generation increases.

The movement of sediment along the stream channel and its delivery to the outlet occurs mainly during intense hydrological events such as flash floods and floods conveying large volumes through suspended, bedload or debris flow transport mechanisms. These events, among other natural processes, are the main drivers of landscape modification and they represent a non-negligible hazard for human activities, settlements and lives. For these reasons, flood events need to be managed through hydraulic structures (D'Agostino, 2013; Piton *et al.*, 2016; Piton and Recking, 2017; Cucchiaro *et al.*, 2019; Marchi *et al.*, 2019). Among several typologies, check dams and bed sills are the most common and widespread engineering solutions to manage and control sediment fluxes during flood events (Cucchiaro *et al.*, 2019; Marchi *et al.*, 2019). The European Alps faced an expansion of this type of control works in the late 19th century. At that time, the intensified pressure of human activities and settlements on mountain watersheds triggered increased rates of erosion processes and slope instabilities (Marchi *et al.*, 2019). Therefore, the higher supply and transport of sediment along the channel was a factor of high risk for valuable human elements that needed protection (Comiti *et al.*, 2012). As stated by Piton *et al.* (2017), check dams are defined as "*transversal structures built across stream beds and gullies to limit the geomorphic activity of*

torrential watersheds. They can be made of logs, gabions, dry stones, masonry or/and reinforced concrete". The main roles of the check dams, based on Piton *et al.* (2017), are listed as follows:

- bed stabilization: limitation of longitudinal incision and lateral bank erosion caused by torrential flows, prevention of material recruitment and limitation of channel wandering guiding the flow in a designed path;
- hillslope consolidation: control of the activation of hillslopes instabilities limiting the erosion rate of their bottom boundary (i.e., thalweg), re-fill of eroded valleys and slow down of surrounding sediment sources activity;
- slope reduction: creation of an alluvial section in an environment influenced by colluvial processes (i.e., rockfall, landslides) through sediment filling of the upstream reaches, the alluvial section presents a lower slope decreasing flow velocities, limiting bank erosion and controlling sediment transport and boulder mobilization;
- retention: an effect of all the check dams with the spillway built higher than the stream bed resulting in the interruption of the sediment continuity; highly efficient measure to trap sediment mobilized by flood events;
- sediment transport regulation: change of sediment dynamics through the creation of fixed points with buffer compartments between check dams in which sediment is stored and gradually released; fixed points also stop headward propagating erosion processes.

The design of the check dams is based on their aforementioned roles to effectively stabilize the channel, retaining sediment and preventing an excess of erosion that might destabilize the surrounding hillslopes. However, their design for flood control is based on the evaluation of their efficiency at local and event scale and frequently it does not consider their long-term impact on the whole system's sediment dynamics (both hillslope-channel and in-channel sediment transfers) (Cucchiaro *et al.*, 2019). In fact, check dams are designed to accomplish at least one objective but their impacts could have several effects both in the location of the control work and beyond (Lucas-Borja *et al.*, 2021). Moreover, the efficiency of the check dam systems in relation to their functions is ensured only if the control works are properly maintained (Marchi *et al.*, 2019; Lucas-Borja *et al.*, 2021). Indeed, check dams represent a measure to control sediment yield but their effects tend to progressively diminish over time due to sediment filling., especially in highly dynamic mountain streams. Hence, when not properly designed and/or not well maintained, check dams systems are observed to have a very low effect against flash flood impacts (Lucas-Borja *et al.*, 2021). However, filled check dams that are not effective any more in controlling flash floods may play a hillslope consolidation role (Piton *et al.*, 2017; Lucas-Borja *et al.*, 2021). At the same time, in some cases check dams can produce undesired effects. Among these lasts, the channel scouring downstream of

the control works due to the erosive power of the free fall is one of the most observed critical issues. If not prevented or controlled, the local scouring can result in instabilities of the check dams and, eventually, in their collapse with the release of the sediment stored over time (Gellis *et al.*, 1995; Lucas-Borja *et al.*, 2021). Therefore, the assessment of the impacts of check dams on sediment dynamics in mountain streams is of major importance for the maintenance of the existing control structures and for the designing of new ones (Marchi *et al.*, 2019).

The aforementioned issues can be assessed through the adoption of integrated approaches that include the combination of remote sensing and field survey data analysis. This is possible thanks to the advances in survey technologies that allow the rapid acquisition of data at high spatial resolution (Heritage and Hetherington, 2007). Spatially-distributed and morphologically-based attributes can be captured by a wide range of techniques. One of them is airborne Light Detection and Ranging (LiDAR): a remote sensing technology that uses a pulsed laser to measure object's variable distance from the earth surface (Devereux and Amable, 2009). In the last decade, the wide use of LiDAR technology in the geomorphology community permitted to analyse landslides, river channel networks, river beds morphology and allowed the quantification of sediment erosion and deposition in detailed flood modelling (Tarolli, 2014). However, the frequency of LiDAR surveys is often limited by its relatively high cost (Cucchiaro *et al.*, 2019). In any case, LiDAR is able to acquire High-Resolution Topography (HRT) data of earth surface (Tarolli, 2014). As stated by Lague and Felmann (2020), HRT data are characterized by "*a typical combination of four characteristics: they are three dimensional, high resolution, high precision and synoptic*". Furthermore, HRT data can be handled by software platforms (i.e. Geographic Information System, GIS) that permit different elaborations including Digital Elevation Models (DEMs) and Digital Terrain Models (DTMs) (Lane *et al*., 2003; Tarolli, 2014). DEMs generally take into account all the objects present on the ground (i.e., vegetation, buildings) whilst DTMs represent the bare ground surface filtered from vegetation, forest cover and other surface objects. Moreover, DTMs not only represent the relief, but also report its description in terms of slope, contour lines, peaks, ridges, including anthropic breaklines (control works, roads, railways) (Podobnikar *et al*., 2000). Through the geomorphological modelization based on HRT data accounting for different years, it is possible to prioritize the maintenance and the management of the control works in a torrential watershed (Cucchiaro *et al.*, 2019). Different studies analyzed the bed material conveyed by stream flow and stored behind check dams in order to estimate erosion and deposition rates. The stored sediment is considered as a record of environmental changes and provide data for the quantification of geomorphological processes (Romero-Diaz *et al.*, 2007; Bussi *et al.* 2013; Wang *et al.*, 2014; Rodriguez-Lloveras *et al.*, 2015; Lucas-Borja *et al.*, 2021). Victoriano *et al.* (2018) evaluated the geomorphic impacts of hydraulic structures in the Portainé

mountain catchment in Spain, analyzing the bed material retained by a system of control works. The multi-temporal analysis of DEMs obtained from LiDAR surveys accounting for 7 years attested the occurrence of several erosion processes in different reaches and patterns of deposition located mainly upstream of the channel control works. Therefore, the analysis offered quantitative estimations of sediment erosion and deposition processes in the basin and allowed the evaluation of the conditions of engineering hydraulic structures along the channel network. The assessment of the morphological dynamics of mountain basins is increasingly focusing on quantitative estimations to identify geomorphic changes through time. Erosion and deposition processes can be detected comparing DTMs of different years through the DEM of Difference (DoD) approach, where patterns of erosion and deposition can be visually recognized and quantified (Lane *et al*., 2003; James *et al.*, 2012) and, as stated by Wheaton *et al*. (2009), to "*estimate the net change in storage terms for morphological sediment budgets*". However, the DoDs are often affected by variable uncertainties that result in inaccurate quantifications of eroded and deposited sediment volumes (Wheaton, 2008). The uncertainty in the DoDs can be related to a vast array of sources, especially to the errors in the DTMs (i.e., point quality, sampling methods, surface composition, topographic complexity) (Wechsler, 2003; Wechsler and Kroll, 2006). Nevertheless, it can be evaluated through the application of the method presented by Wheaton *et al.* (2009), which is based on a Fuzzy Inference System (FIS) that allows to combine singular errors from different sources (Wheaton *et al.*, 2009). The DoD is a widely applied method in mountain basins. Cavalli *et al.* (2017) developed DoDs based on FIS methodology using two subsequent DTMs for 2005 and 2011 derived from airborne LiDAR data to detect topographic changes caused by erosion, transport and deposition in two adjacent alpine basins, Gadria and Strimm, located in the Venosta valley (BZ), Italy. The catchments were chosen for their consistent different morphology and because of their different types and intensity of sediment transfer processes. The comparison between the DTMs permitted the investigation of the role of topography on sediment erosion and deposition and to describe the influence of debris flows and fluvial processes on the morphology of the two basins. Their research resulted in the volumetric quantification of changes in the two catchments and allowed their visual comparison in terms of erosion and deposition patterns. The Gadria Torrent basin presented well defined and discriminated erosion and deposition clusters, on the contrary, in the Strimm Torrent basin, an overlap of eroded and deposited sections was observed. The consistent results of the DoDs were then compared with post-event field surveys estimates leading to congruous conclusions, encouraging the adoption of an integrated approach of the two methods. A wide literature on DoDs applications is present, hereafter we cite the research presented by Bezak *et al.* (2017), with a multi-temporal analysis of the geomorphic responses of the Kuzlovec basin in central Slovenia to the 2014 extreme flash flood, and by Pellegrini *et al.*, (2021),

who assessed the erosion and deposition processes in the Tegnas alpine catchment, Italy, caused by the 2018 Large Infrequent Disturbance (LID): the storm named "Vaia".

In this thesis, the sediment dynamics of Vegliato Torrent (UD), where several hydraulic structures were built in the last decades, are quantified through a multi-temporal analysis. The main objective of this work is to define the efficiency of the control works system and its effects on sediment dynamics in a steep channel affected by a flash flood in 2021. To achieve this objective, multi-temporal DTMs derived from LiDAR surveys data (2019 and 2022) are used to compute DoDs to detect and quantify the amount of sediment eroded and deposited during the flash flood event. The specific objectives are listed as follows: 1) assessment of the structural condition and functionality of the check dams and bed sills built within the main channel through the creation of a database derived from field surveys data; 2) analysis of the grainsize distribution of the bed material for the entire channel network and for several check dams through data series sampled during the field surveys; 3) characterization of the rainfall event that triggered the 2021 flash flood; 4) generation of robust DoDs with the application of the FIS methodology to analyze and quantify geomorphic changes caused by the 2021 flash flood.

2. Materials and methods

2.1 Study area

The Vegliato Torrent basin (Fig. 1) is located in the municipality of Gemona del Friuli (UD) and it extends for around 5 km^2. The basin is comprehended between Mount Chiampon (1709 m a.s.l.), Mount Deneal (1701 m a.s.l.) and Mount Cuarnan (1372 m a.s.l.), which are part of the Julian Prealps. The Vegliato Torrent flows into the Ledra River, a tributary of Tagliamento River. The Vegliato Torrent catchment is closed at the outlet at 355 m a.s.l. The mean annual precipitation in the catchment amounts to 2130 mm with intense precipitation events frequently observed during the summer season and persistent rainfall in autumn (2000 – 2021; arpaFVG). The main lithology that characterizes the basin is dolomitic and it is directly attributable to the origin of the torrent in the southern slope of Mount Chiampon (Coccolo and Sgobino, 1996). Moreover, the catchment is composed by carbonate rocks from the Late Triassic – Cretaceous and by *Flysch of Grivò* (Zanferrari *et al.*, 2011).

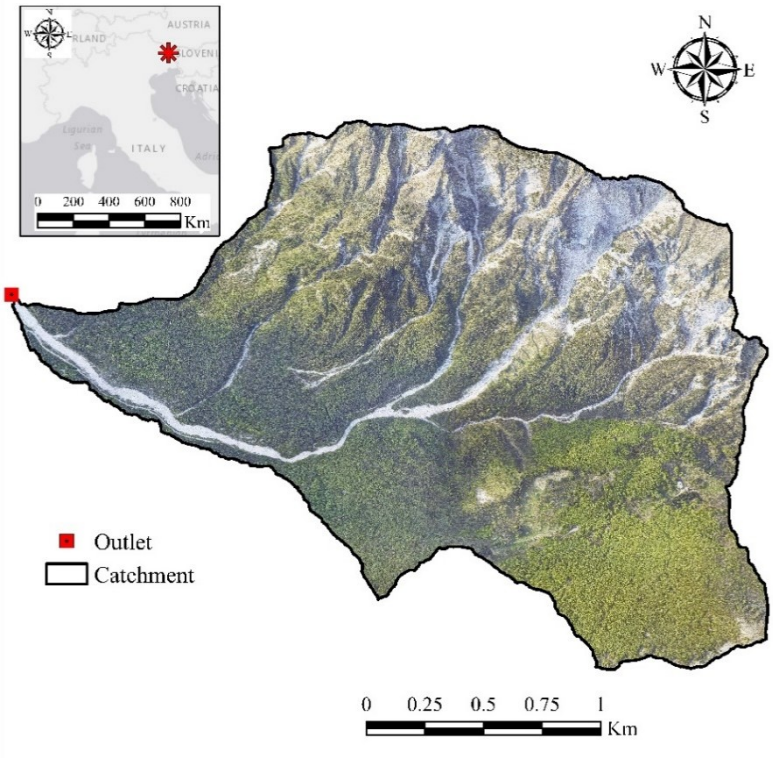

Figure 1: the Vegliato Torrent basin located in Gemona del Friuli (UD), in the North East of Italy.

The basin presents a complex topography with an average slope of 35° (Fig. 2). The highest slope grades are observable in the south-facing part of the basin, where the channel network develops along the impervious hillslopes of Mount Chiampon. The basin is widely covered by spruce (*Picea abies*), beech (*Fagus sylvatica*), scots pine (*Pinus sylvestris*) and black pine (*Pinus nigra*) forests. A consistent portion of the basin is covered by bare rock, especially at the highest altitudes of M. Chiampon and M. Deneal hillslopes, where a little portion of the catchment also presents grassland. In the basin, the main channel is 2.7 km long and it is characterized by a straight channel with cobbles and boulders (based on the morphological classification proposed by Billi, 1994), presents an average slope equal to 25° and a mean bankfull width of 29.3 m. The catchment is characterized by the presence of a widespread system of channel control works. Along the channel, 20 check dams and two bed sills are registered by the Regional Cadastre of hydraulic structures built by Friuli Venezia Giulia (IRDAT, 2018). The study area for the accomplishment of the objectives of this study is limited to the section of the channel network where the control works are located. The control works are located mainly in the main channel but there are several structures also within tree tributaries. One of them is in the downstream part, the other two are located in the middle section of the channel network and in the upstream part, respectively (Fig. 3). Within the study area, three areas of interest are defined for further analyses regarding grainsize distribution and morphological changes, and are named Reach-1, Reach-2 and Reach-3 (hereinafter R1, R2, R3), respectively (Fig. 4). R1 is in the upper

section of the main channel and is 880 m long. It presents an average slope of 30° and it is located in the south-facing hillslopes of M. Chiampon, where the topography is the most complex. R2 is located in the middle section of the channel network, it measures 440 m in length and exhibits an average slope of 25°. R3 is located near the outlet, it is 550 m long and presents a milder slope equal to 16° and a plane bed morphology. The main features of the Vegliato Torrent basin, the main channel and the three reaches are summarized in Table 1.

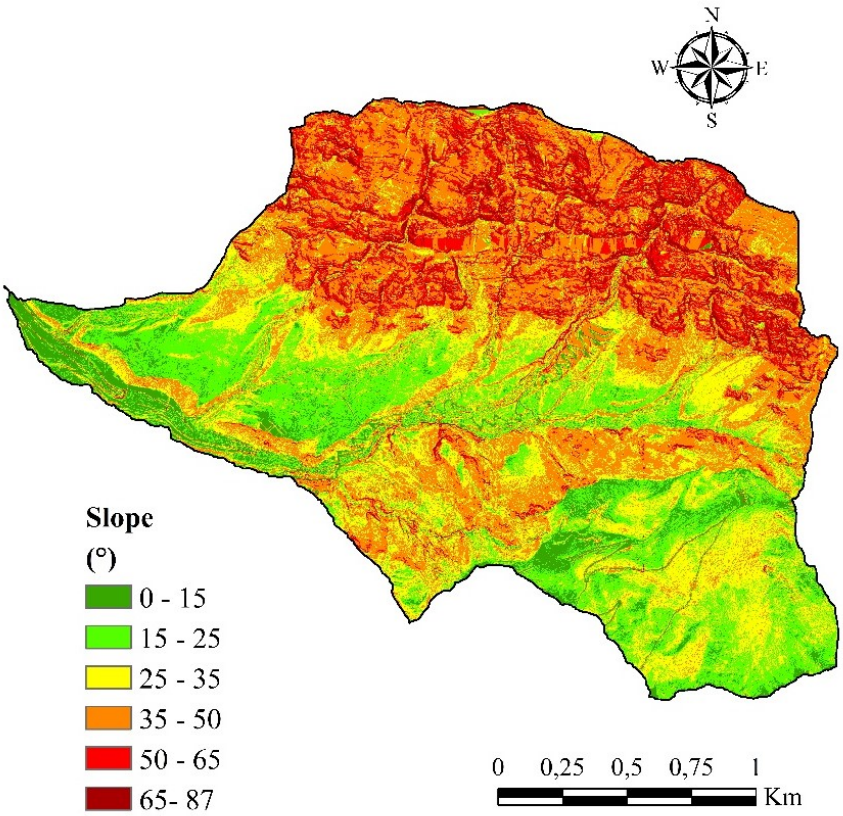

Figure 2: slope gradient of the Vegliato Torrent basin. The average slope is 35°.

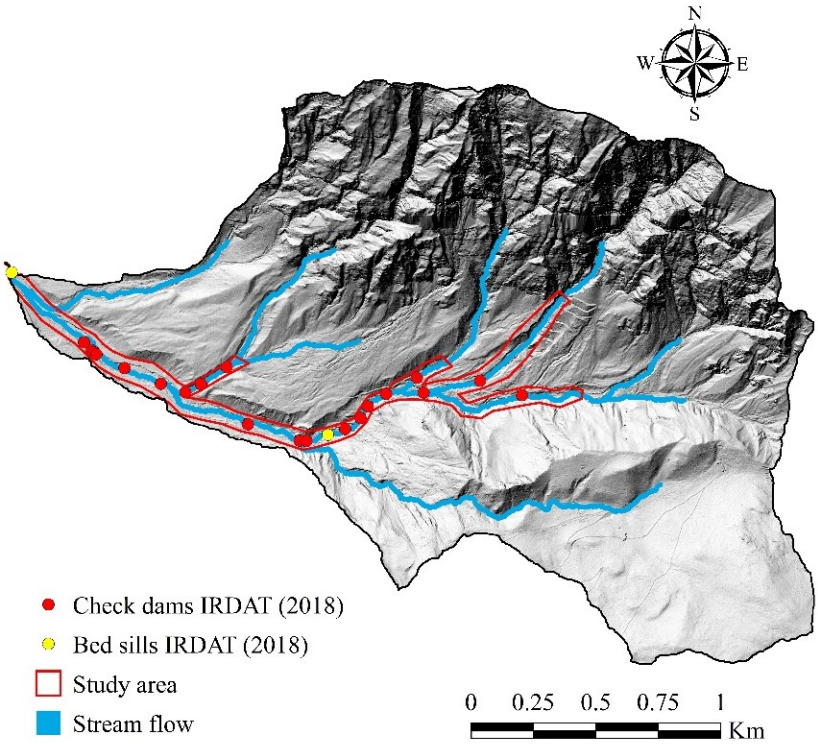

Figure 3: The stream flow, the control works registered in IRDAT (2018) and the study area in the Vegliato Torrent basin.

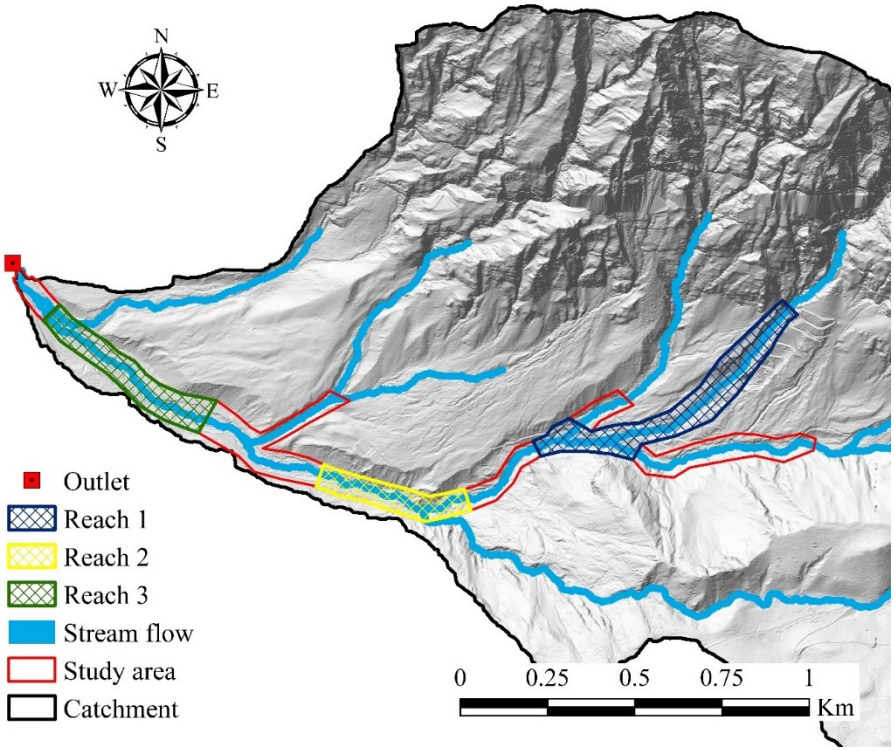

Figure 4: The channel section representing the study area and the three reaches.

Table 1: Main topographic, climatic and geomorphological features of the Vegliato Torrent basin.

Vegliato Torrent		
Basin	Area (Km^2)	5
	Max. altitude (m a.s.l.)	1709
	Min. altitude, outlet (m a.s.l.)	355
	Altitude drop (m)	1354
	Average slope (°)	35
	Mean annual precipitation (mm)	2130
Channel network	Length (Km)	2.7
	Average slope (°)	25
	Mean bankfull width (m)	29.3
	Morphology	Straight channel with cobbles and boulders / cascade
R1	Length (m)	880
	Average slope (°)	30
R2	Length (m)	440
	Average slope (°)	25
R3	Length (m)	550
	Average slope (°)	16
Control works (IRDAT, 2018)	Check dams	20
	Bed sills	2

The Vegliato Torrent is in dry conditions for the most part of the year, except for the streamflow observed during persistent or intense rainfall events (De Marco *et al.*, 2021). Recent major events are reported by Coccolo and Sgobino (1996). On September 15th 1976, after the earthquake of 6.5 magnitude (Richter scale) that deeply affected the entire Friuli-Venezia Giulia region, a massive landslide of 250000 m^3 in volume originated in the hillslopes of Mount Chiampon and Mount Deneal entered into the channel and, during the following floods, a series of debris flows were generated. Particularly, the most critical were registered during the rainfall events on October 12th 1976 with 70 mm in 3 hours and on August 2nd 1983 with 106 mm in 3 hours. On June 9th 1987, an extraordinary flood event generated by heavy rainfall of 125 mm mobilized a sediment volume estimated to 80000 m^3, of which at least 45000 m^3 moved downstream destroying the two bridges of the forest road and heavily damaging some of the existent check dams. Over time, these events and the effects of the control works present within the stream channel majorly contributed to the morphological aspects of the Torrent visible nowadays.

2.2 Control works system assessment

The location of the control works in the Vegliato Torrent channel has been registered through GPS coordinates during the field survey conducted in summer 2022. The assessment of the conditions of the control works took into consideration the dimensions of each check dam/bed sill and their structural functionality. To assess the conditions of the control works system, the database is classified through different attributes. Each control work is featured by 1) an identification number, 2) an identification alpha-numerical code, 3) X and Y coordinates, 4) the typology of hydraulic structure (check dam, filtering check dam, bed sill), 5) realization year, 6) dimensions (height, width in m, only for check dams), 7) state (good, damaged, destroyed), 8) functionality (operative, compromised, null) and 9) an annotation class to describe critical features worth to be considered such as location and description of structural damages, presence of sediment over-flood, sediment filling and/or outflank of the control work.

In order to obtain an estimation of the net efficiency of the control works system based on the field surveys data, an efficiency value is assigned to each hydraulic structure. To assess the efficiency of each control work, the state and functionality classes are converted into numerical values based on the following scheme:

- State: good = 1 (the structure does not present structural damages);
- Damaged = 0.5 (presence of one or several structural damages, i.e., damaged spillway);
- Destroyed = 0 (the structure is extremely damaged, i.e., only a small section is still present)
- Functionality: operative = 1 (the structure accomplishes the functions for which is designed);
- Compromised = 0.5 (the functions are only partially accomplished due to one or different causes, i.e., sediment over-flooding);
- Null = 0 (the structure is not functional anymore due to one or several causes, i.e., complete filling).

The efficiency of each control work results from the mean of the two values assigned to each structure. For example, a control work in good state and compromised functionality (values 1 and 0.5, respectively) exhibits a net efficiency of 75%. Each control work presenting a null functionality, independently from their structural state, is arbitrarily given a null efficiency value because of their inherent incapability to accomplish any objective they are designed for. This protocol is based on qualitative observations and aims to generally estimate the efficiency of the control works system through the field survey data collection.

2.3 Grain size distribution

To determine the characteristics of the sediment in the Vegliato Torrent, grain size data were sampled during the field surveys. The measurement of the grains took place within the main channel of the torrent, nearby 14 check dams located in the study area. Grain size data series were collected in mm by applying a linear transect method in the direction of the bankfull width of the channel, spacing every measurement by 1 meter (two times the D_{max}). Therefore, the grain size of each check dam is represented by a series of 60 data (30 samples upstream and 30 downstream of the control work) for a total dataset of 840 measurements for the study area. Furthermore, the characterization of the grainsize of three check dams located respectively in the three areas of interest is reported in detail. The analysis is accomplished both upstream and downstream of the hydraulic structure and the respective distributions are represented by a code that will be use hereinafter. The codes are as follows:

- R1: Grainsize distribution upstream of check dam 25 (GS25U);
  Grainsize distribution downstream of check dam 25 (GS25D);
- R2: Grainsize distribution upstream of check dam 15 (GS15U);
  Grainsize distribution downstream of check dam 15 (GS15D);
- R3: Grainsize distribution upstream of check dam 3_4_5 (GS3_4_5U);
  Grainsize distribution downstream of check dam 3_4_5 (GS3_4_5D).

The grain size distribution and its characterization for the check dams and for the study area is determined with the classification of the dataset in *phi* (Φ) classes with 0.5 range and the determination of the relative frequency f (%) and cumulative frequency F_c (%). To these aims, the following equations are applied:

$$\Phi = -\log_2 D \quad (1)$$

$$f = (n / N) * 100 \quad (2)$$

$$F_c = f_i + F_{ci-1} \quad (3)$$

In Equation 1, D represents the grain size expressed in mm. Equation 2 is determined by the absolute frequency for each class n and the total data series N. The computation of F_c (Eq. 3) results from the sum of the relative frequency of a class f_i and the cumulative frequency of the previous class F_{ci-1}.

The features of the stream bed material in the study area are evaluated through the determination of main diameters D_{10}, D_{16}, D_{30}, D_{40}, D_{50}, D_{84}, D_{90}. To calculate the main diameters D_x, Φ_x classes related to each main diameter are computed:

$$\Phi_x = E_{x-1} + \frac{E_x - E_{x-1}}{F_{cx} - F_{cx-1}} * (x - F_{cx-1}) \tag{4}$$

then,

$$D_x = 2^{-\Phi_x} \tag{5}$$

In Equation 4:

- E_x: highest extreme of the subsequent Φ_x class;
- E_{x-1}: highest extreme of the precedent Φ_x class;
- F_{cx}: cumulative frequency of the subsequent Φ_x class;
- F_{cx-1}: cumulative frequency of the precedent Φ_x class;
- *x:* % class of the main diameter.

The characterization of the grain size through the main diameters permits to evaluate whether the stream bed sediment is homogenous or heterogeneous. To this aim, the Standard Deviation of the dataset, expressed by the σ index, is determined through Equation 6. Given the threshold of 1.35 for this study case, the grain size presents an homogenous distribution if $\sigma < 1.35$, on the contrary, the distribution results heterogeneous if $\sigma > 1.35$.

$$\sigma = \sqrt{\frac{D_{84}}{D_{16}}} \tag{6}$$

2.4 Rainfall data

The Vegliato Torrent basin is frequently affected by sudden rain events that may cause an increase in discharge and in sediment transport. During the study period (2019-2022), many changes in the morphology of the basin occurred due to the high amount of yearly precipitation and heavy rainfall events. However, the flash flood that affected the catchment on July 30th 2021 (Fig. 5) can be considered the main event which heavily impacted on its morphological features in recent time. The

rainfall data of the event were recorded every minute by a rain gauge with an accuracy of 0.2 mm located in the meteorological station of Gemona del Friuli (UD) (Cazorzi, data not published). The return time of the rainfall event is estimated through the application of the Depth-Duration Frequency model for the Friuli Venezia Giulia Region (Cazorzi, data not published). The accuracy of the data permits to determine the maximum rainfall intensities for 5, 10, 15, 30 minutes and 1 hour (respectively named I_{5min}, I_{10min} I_{15min}, I_{30min}, I_{1h},).

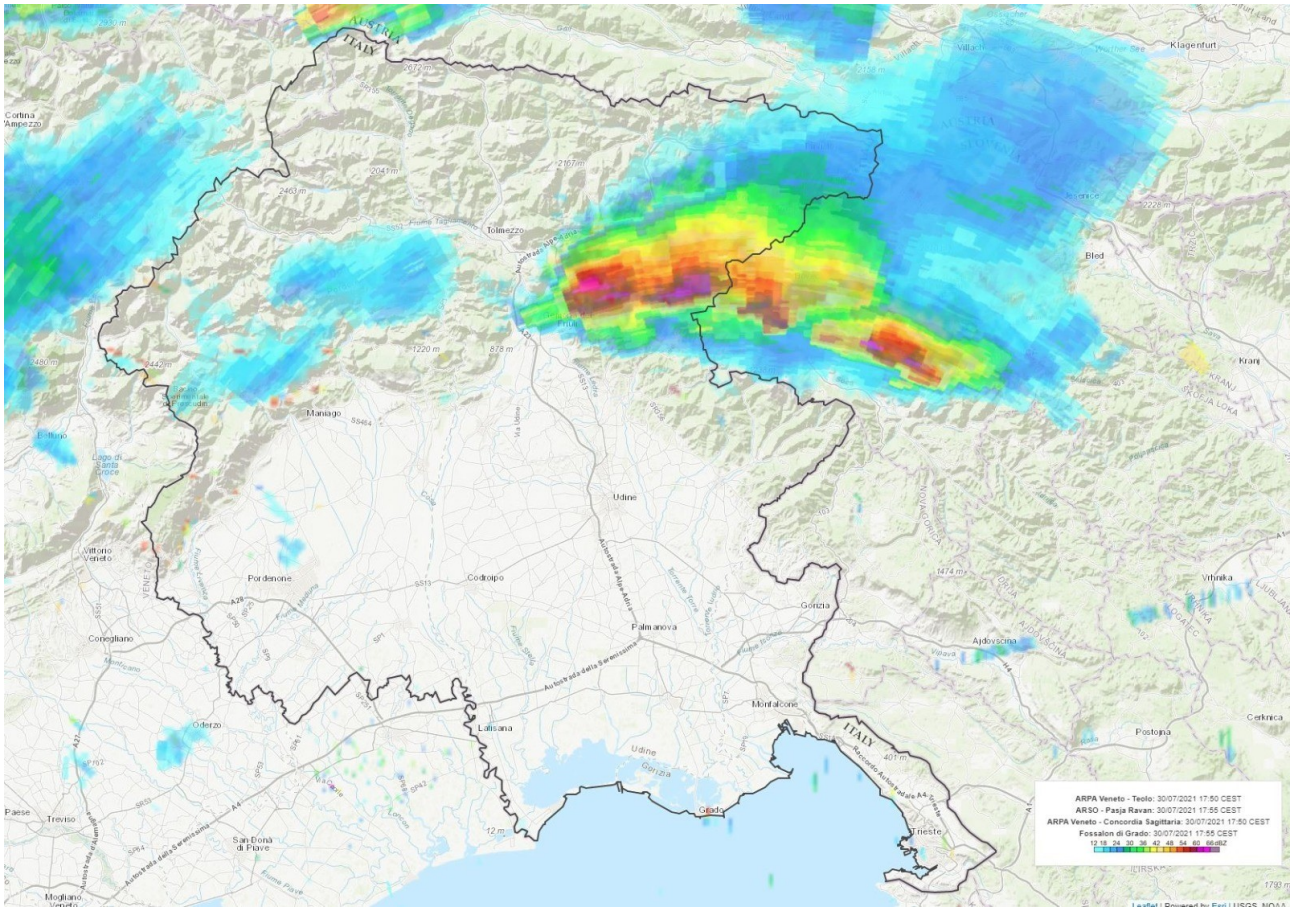

Figure 5: Radar view of the July 30th 2021 rain event on the Friuli Venezia-Giulia Region. The precipitation intensity on the Vegliato Torrent catchment at 17:50 CEST overtakes 66 dBZ, equivalent to 3 mm h^{-1} (Image by Arpa Veneto, radar Teolo (PD)).

2.5 Geomorphic change detection

The changes in the bankfull width of the channel network caused by the 2021 flash flood are determined through the measurement of the mean bankfull width of the Vegliato Torrent in 2019 and 2022. Through ESRI's Arcgis, 40 bankfull width measurements along the channel networks are registered for each year from the 2019 and 2022 orthophotos.

The geomorphic changes occurred due to the impact of the 2021 flash flood are determined through the application of the DoD methodology. The analysis aims to compare the topographic

differences between the 2019 and 2022 DTMs. The two DTMs (1 m resolution) were generated by interpolation of filtered point clouds obtained through LiDAR surveys carried out by private companies. To this end, Geomorphic Change Detection 7.5.0.0 AddIn (Wheaton *et al.*, 2009) for ESRI's Arcgis is used to subtract the old-2019 DTM to the new-2022 DTM. The methodology proposed by Wheaton *et al.* (2009) allows the detection of real geomorphic changes weighted from fictitious differences resulting from noise and it is based on the evaluation of the spatially distributed elevation uncertainty. The proposed methodology for the application of the DoD is mainly constituted by three steps: 1) computation of the DEM elevation uncertainty on individual cells using the FIS; 2) propagation of the uncertainty into the DoD, still on cell-by-cell basis; 3) use of a probabilistic threshold to define the statistical significance of the propagated uncertainty.

The first computation is carried out using the FIS, which derives an uncertainty value (output) using known information about the morphological settings and the survey characteristics (input). The FIS is constituted by four main components: specification of FIS type, definition of fuzzy membership functions (MFs) for the inputs, definition of rules linking inputs and outputs and definition of MFs for the output. The procedure results in a crisp, single value of elevation uncertainty for each cell (Wheaton *et al.*; 2009). In this thesis, two inputs are used: slope and point density, respectively utilized as proxies for uncertainty related to topographic complexity and survey accuracy (Wheaton *et al.*, 2013). The input variables are classified into two MFs (Low, High) by setting ranges for each class of the inputs, taking into account the study area characteristics. The relation between input and output is defined through four rules. Then, three MFs for the output (Low, Medium, High) are defined to categorize the elevation uncertainty δz. The ad-hoc FIS defined for this study is reported in the following table:

Table 2: input variables (slope and point density) and output (elevation uncertainty δz) with the respective ranges defining the MFs used in the ad-hoc FIS for the computation of the DoD 2022 - 2019 in the Vegliato Torrent.

		Slope (%)	
		Low (0; 0; 12.5; 25)	High (25; 35; 45; 90)
Point density (pt m^{-2})	Low (0; 0; 22; 104)	Medium δz (0.1; 0.2; 0.3; 0.4)	High δz (0.4; 0.5; 0.55; 0.63
	High (22; 104; 180; 240)	Low δz (0; 0; 0.1; 0.2)	Medium δz (0.1; 0.2; 0.3; 0.4)

The second step is tackled applying the error formula proposed by Brasington *et al.* (2000) (Eq, 7) and allows to combine the spatially distributed errors of the two DEMs.

$$\delta u_{DoD} = \sqrt{\left(\delta Z_{DEMnew}\right)^2 + \left(\delta Z_{DEMold}\right)^2} \tag{7}$$

in which, δu_{DoD} is the propagated error in the DoD, δZ_{DEMnew} and δZ_{DEMold} are the elevation uncertainty in the new and old DEM, respectively.

The third step consists in the setting of a probabilistic threshold to validate the real topographic changes. The threshold is set by choosing the corresponding *t-value* derived according to the Equation 8. The choice of the probabilistic threshold is based on Brasington *et al.* (2003) and Lane *et al.* (2003).

$$t = \frac{\left|Z_{DEMnew} - Z_{DEMold}\right|}{\delta u_{DoD}} \tag{8}$$

in which, Z_{DEMnew} - Z_{DEMold} is the absolute result of cell-by-cell DoD and δu_{DoD} is the propagated error computed in the second step. In this thesis, a 95% confidence interval (*t-value* equal to 1.96) is chosen in order to conservatively detect the minimum volume of sediment eroded and deposited. The DoDs aim to investigate the geomorphic changes occurred in the 2.7 km long active channel of the Vegliato Torrent and, thus, to assess the response of the control works system to the flash flood event. Furthermore, the sediment budget segregation is performed in three segregation areas (R1, R2 and R3), defined to analyze important patterns of topographic differences, sediment mobilization and deposition in detail.

3. Results

3.1 Control works system assessment

. The total number of hydraulic structures assessed in the field survey amounts to 31, counting 24 check dams and 7 bed sills (Fig. 6). The control works are built within the main channel and in three tributaries. In the main channel, a total number of 22 control works is present (check dams 2 to 8, 15 to17, 19 to 23, 25 and the 7 bed sills). The tributary in the downstream part of the channel network is located between check dam 8 and 15 and counts 6 check dams (9 to 14), whilst in the middle and upstream sections, the other two tributaries are characterized by the presence of only one check dam each, the 24 for the tributary located between the check dams 23 and 25 and the 27 for the tributary located between the bed sills 26 and 28. The majority of the control works was built in 1980 (14 out of 31) and a minor part in 1930 (6) and 1950 (2). However, the building date of almost 30%

of the assessed structures (9 out of 31) is unknown because they are not dated in the regional cadastre (IRDAT, 2018). Almost the entire system of control works is constituted of reinforced concrete, masonry and stones structures (20 check dams and the 7 bed sills), except for a minor part which comprehend four wooden check dams. The mean height and width of the hydraulic structures is 4 m and 28 m, respectively.

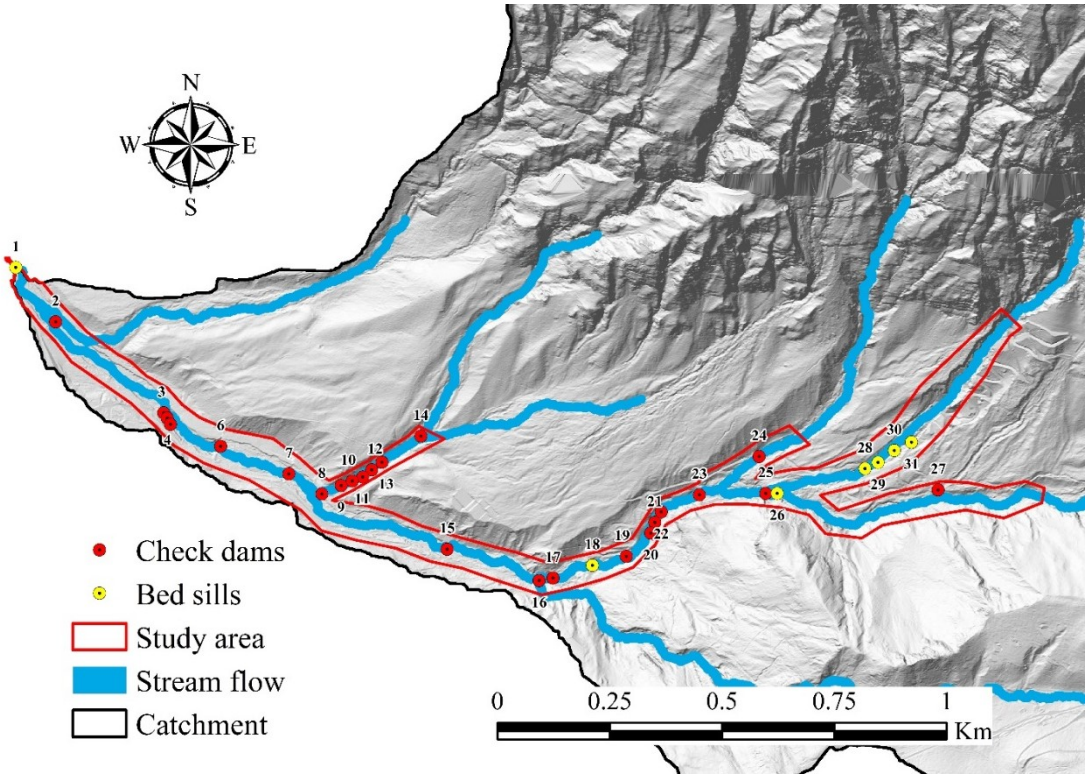

Figure 6: the control works system in the Vegliato Torrent basin comprehends 24 check dams and 7 bed sills.

The system presents 12 control works in good structural state (39%), 8 damaged structures (26%) and 11 destroyed elements (35%) (Fig. 7). The damaged check dams are several and exhibit damages to the lateral wings, sides, spillways and buttresses and decay of the wooden components (Fig. 8). Considering the functionality, only two are still operative (6%) whilst 11 exhibit compromised functionality (35%) and 18 do not accomplish any function (58%) (Fig. 9).

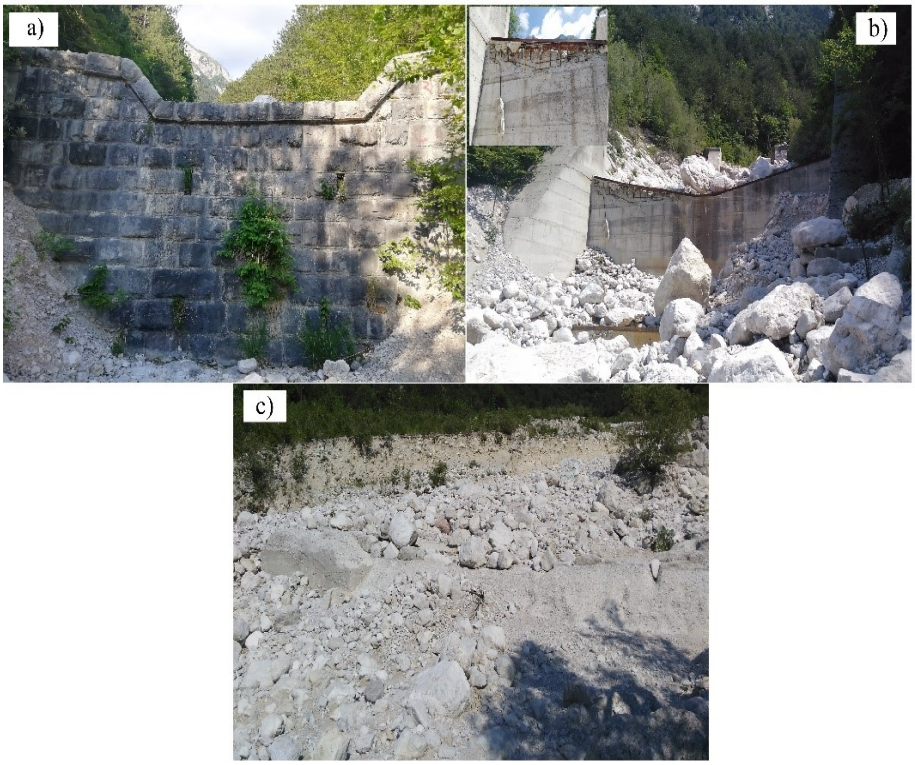

Figure 7: three control works in different structural states: a) the check dam 9 (ID F-11874-1-1) is in good conditions; b) the check dam 20 (ID F-11869-6-6) presents a damaged spillway, c) the check dam 3 (ID F-11869-4-2) is destroyed.

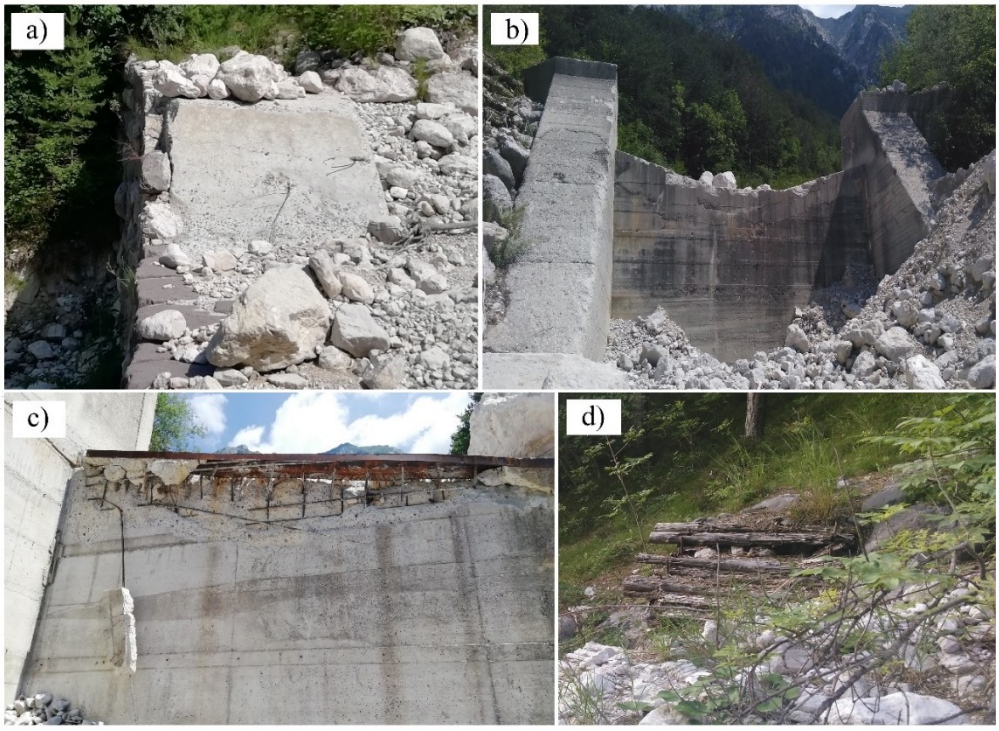

Figure 8: damages observed in some control works: a) the check dam 17 (ID F-11869-5-4) is damaged on the right wing; b) the check dam 22 (ID F-11869-6-7) presents structural damages to the concrete, c) the damaged spillway of the check dam 20 (ID F-11869-6-6); d) wood decay of the check dam 13 (ID F-11874-1-5).

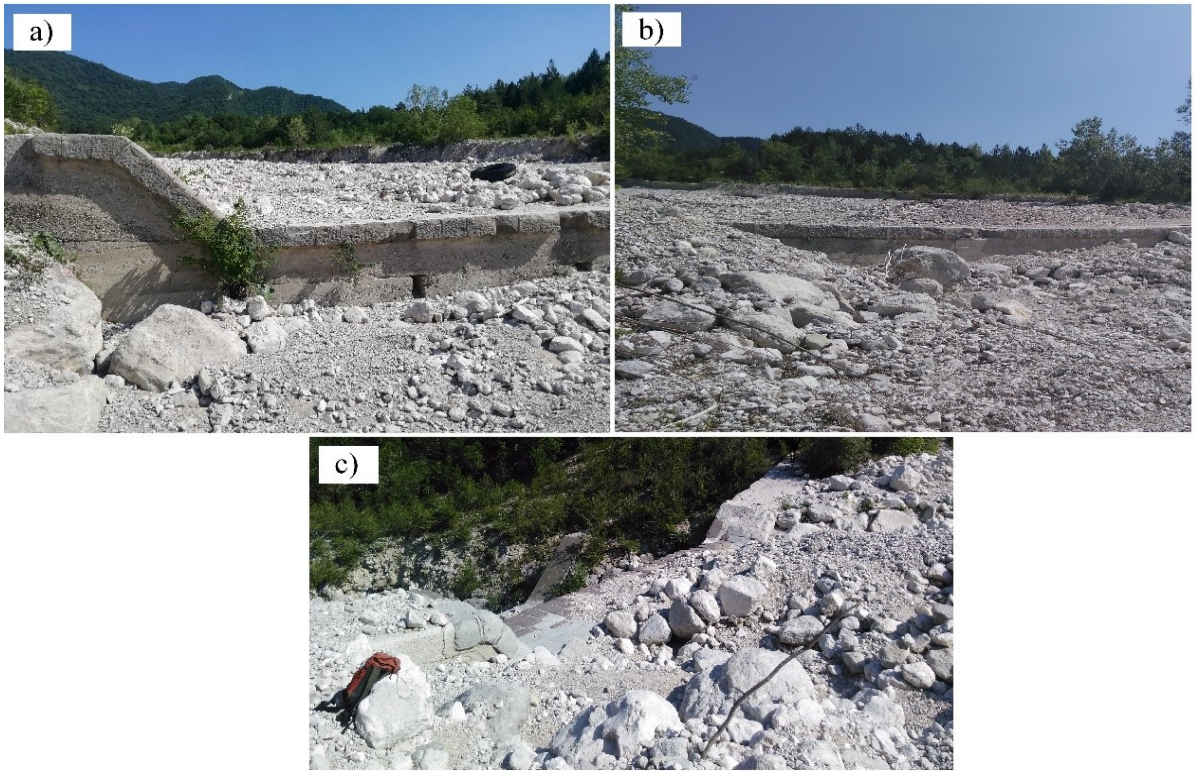

Figure 9: three control works with different functionality levels: a) the check dam 2 (ID F-11869-3-6) is operative; b) the fordable bed sill 1 (ID F-11869-3-4) presents a compromised functionality due to partial sediment over-flooding, c) the check dam 15 (ID F-11869-5-1) is not functional by any means due to complete sediment filling.

Several structures present critical issues such as sediment over-flooding (17 control works) (Fig. 10), outflanking on one side or in both sides (4) and sediment filling (4) (Fig. 11). One check dam presents a severe downstream scour that results in a pensile condition of the structure (Fig. 12). According to the efficiency parameter of the control works based on field surveys data, only two structures present complete efficiency (6%), nine elements partial efficiency (29%) and 17 elements null efficiency (55%). The control works system's net efficiency is estimated in the range of 25 – 30%. The characteristics of the control works system in the Vegliato Torrent basin is summarized in Table 3. For a complete overview of the control works system see Annex 1.

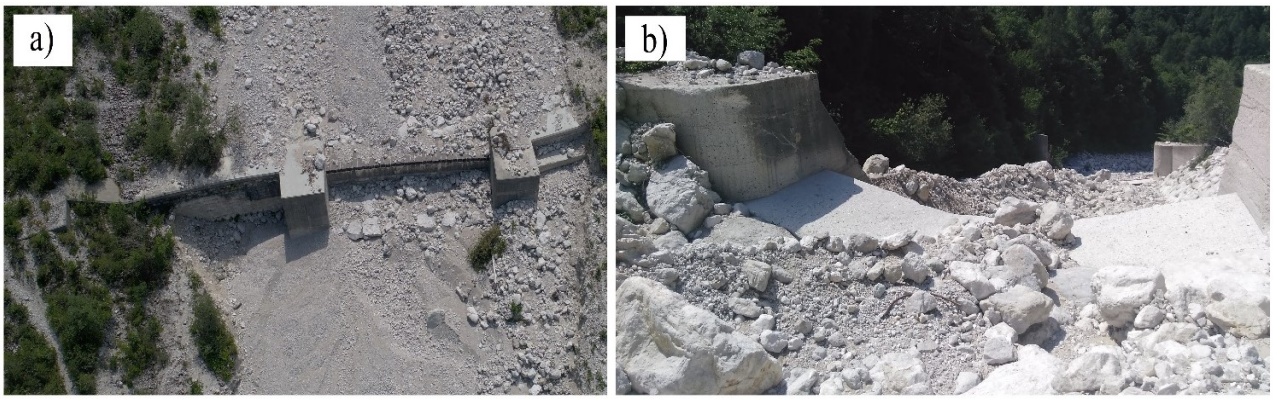

Figure 10: sediment over-flooding in two control works: a) the check dam 7 (ID F-11869-4-6); b) the check dam 22 (ID F-11869-6-7).

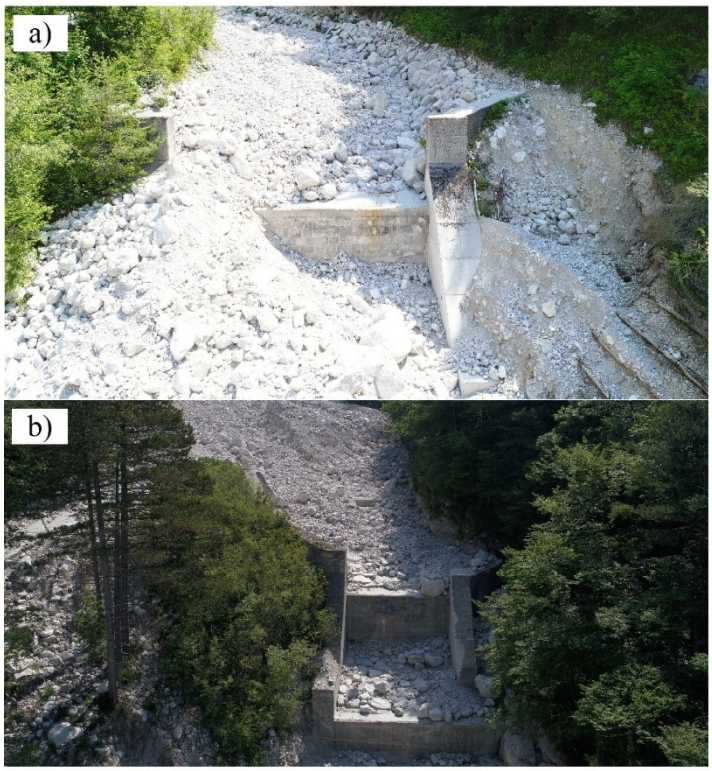

Figure 11: sediment filling and outflanking of two control works: a) the check dam 19 (ID F-11869-6-4) on both sides; b) the check dam 25 (ID F-11869-7-1) on the right side with sediment on the forest road.

Figure 12: severe scour downstream of the pensile check dam 6 (ID F-11869-4-5).

Table 3: assessment of the control works in the Vegliato Torrent basin.

Vegliato Torrent control works system			
		(n)	(%)
Control works	Total count	31	-
Typology	Check dams	24	-
	Bed sills	7	-
Construction year	1930	6	-
	1950	2	-
	1980	14	-
	Unknown	9	-
Material	Concrete, masonry, stones	27	87
	Wooden	4	13
Measurements	Mean height (m)	3.7	-
	Mean widht (m)	28.2	-
State	Good	12	39
	Damaged	8	26
	Destroyed	11	35
Functionality	Operative	2	6
	Compromised	11	35
	Null	18	58
Critical issues	Sediment over-flooded	17	55
	Outflanked	4	13
	Filled	4	13
	Downstream scoured	1	3
Efficiency	Complete	2	6
	Partial	12	39
	Null	17	55
	System net efficiency	-	25 - 30

3.2 Grainsize distribution

The Vegliato Torrent basin presents a grainsize distribution (Fig. 13) mainly represented by Φ classes included between - 4.0 and - 8.5, respectively equivalent to 16 and 360 mm. The most representative Φ class is the - 6.5 – 7.0, equivalent to diameters of 90 – 128 mm, representing the 11.6% of the samples. The second and third most frequent Φ classes are the - 5.5 – 6.0 (45 – 64 mm), accounting for the 11.6% of the sample, and - 6.0 – 6.5 (64 – 90 mm) representing the 10.7%. The median diameter D_{50} is equivalent to 71 mm. The main diameters D_{10}, D_{16}, D_{30}, D_{40}, D_{50}, D_{84}, D_{90} and the mean diameter for the study area are reported in Table 4. The σ index, representing the Standard Deviation of the sample, is equal to 3.42 suggesting a heterogeneous distribution of the bed material.

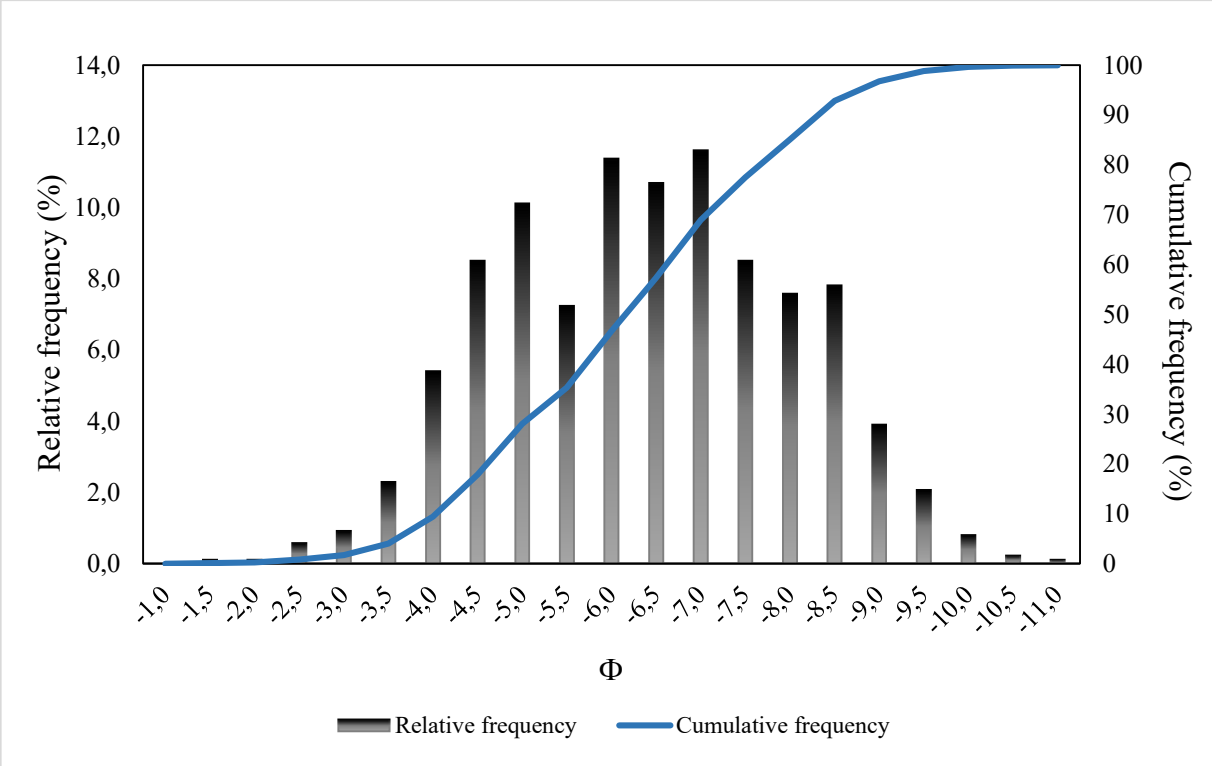

Figure 13: Grainsize distribution curve of the Vegliato Torrent main channel.

Table 4: the main diameters D_{10}, D_{16}, D_{30}, D_{40}, D_{50}, D_{84}, D_{90} and the mean diameter for the Vegliato Torrent main channel.

	Φ	(mm)
D_{10}	-4.02	16
D_{16}	-4.38	21
D_{30}	-5.12	35
D_{40}	-5.70	52
D_{50}	-6.15	71
D_{84}	-7.92	242
D_{90}	-8.31	317
D_m	-6.75	108

For each check dam, D_{50} and σ for upstream and downstream of the structures are computed. The grainsize analysis for each check dam is reported in Annex 2. The grainsize distribution computed for single units exhibits a significant increase of the D_{50} along the channel both downstream and upstream of the check dams. Furthermore, the median diameters are generally higher upstream of the structures (mean of D_{50} equal to 90 mm) than downstream (mean of D_{50} equal to 67 mm) (Fig. 14). The grainsize distribution is observed to be heterogeneous upstream and downstream of all the check dams and it tends to increase along the main channel, even if not in a considerable manner. Furthermore, the heterogeneity reaches peak values in the central section of the study area where check dams 15, 16, 17, 19, 20 and 22 are located. Along the main channel, the upstream sections of the check dams are characterized by a slightly higher heterogeneity (mean of σ equal to 3.08) than in the downstream sections (mean of σ equal to 2.91) but in the most impervious hillslopes of the basin the bed material tends to exhibit almost equal trends of σ (Fig. 15).

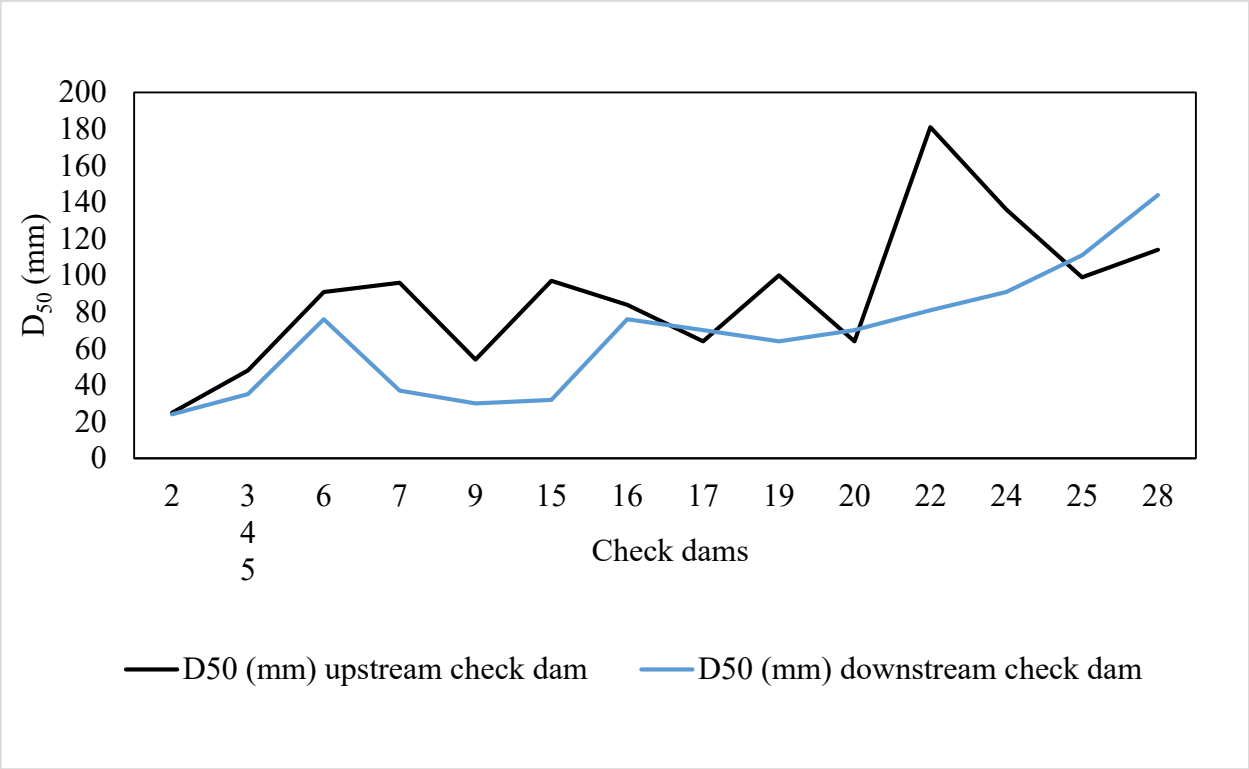

Figure 14: Median diameter upstream and downstream of the check dams in the Vegliato Torrent.

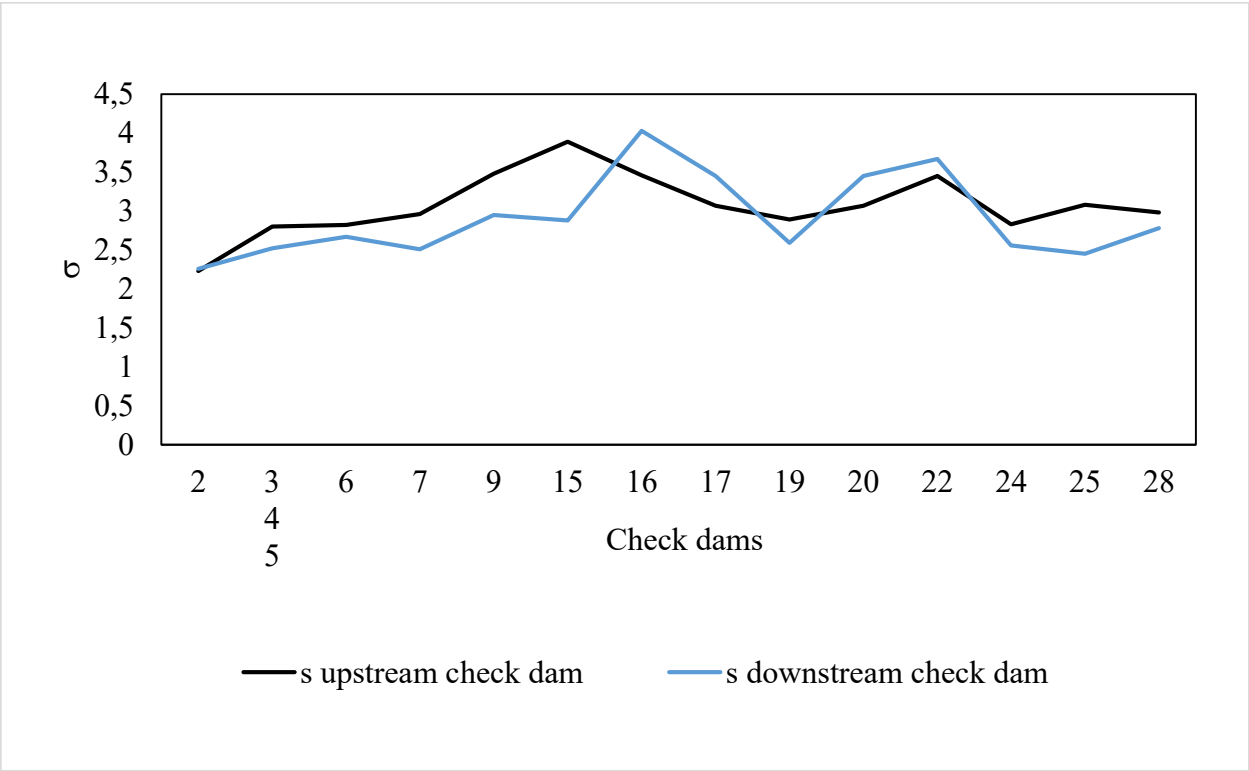

Figure 15: Heterogeneity of the sediment upstream and downstream of the check dams in the Vegliato Torrent.

In Figure 16 the grainsize distributions of check dams 25, 15 and 3_4_5, respectively located in R1, R2 and R3 are reported. The GS25U exhibits a D_{50} equal to 99 mm and a σ of 3.08. The most representative Φ classes are – 6.0 – 6.5 (64 - 90 mm) and – 7.5 – 8.0 (181 - 256 mm). The D_{50} for GS25D is equal to 111 mm and a σ of 2.45. The most representative Φ classes are – 5.5 – 6.0 (45 - 64 mm) and – 6.5 – 7.0 (90 - 128 mm) (Fig. 16a). The GS15U D_{50} is equal to 97 mm and a σ is 3.89. The most representative Φ classes are - 6.5 – 7.0 (90 - 128 mm) and – 8.0 – 8.5 (256 - 360 mm). The D_{50} for GS15D is equal to 32 mm and a σ of 2.88. The most representative Φ classes are – 6.5 – 7.0 (90 - 128 mm) (Fig. 16b). The GS3_4_5U exhibits a D_{50} equal to 48 mm and a σ of 2.80. The most representative Φ classes are – 5.5 – 6.0 (45 - 64 mm). The D_{50} for GS3_4_5U is equal to 35 mm and a σ of 2.52. The most representative Φ classes are – 5.0 – 5.5 (32 - 45 mm) (Fig. 16c).

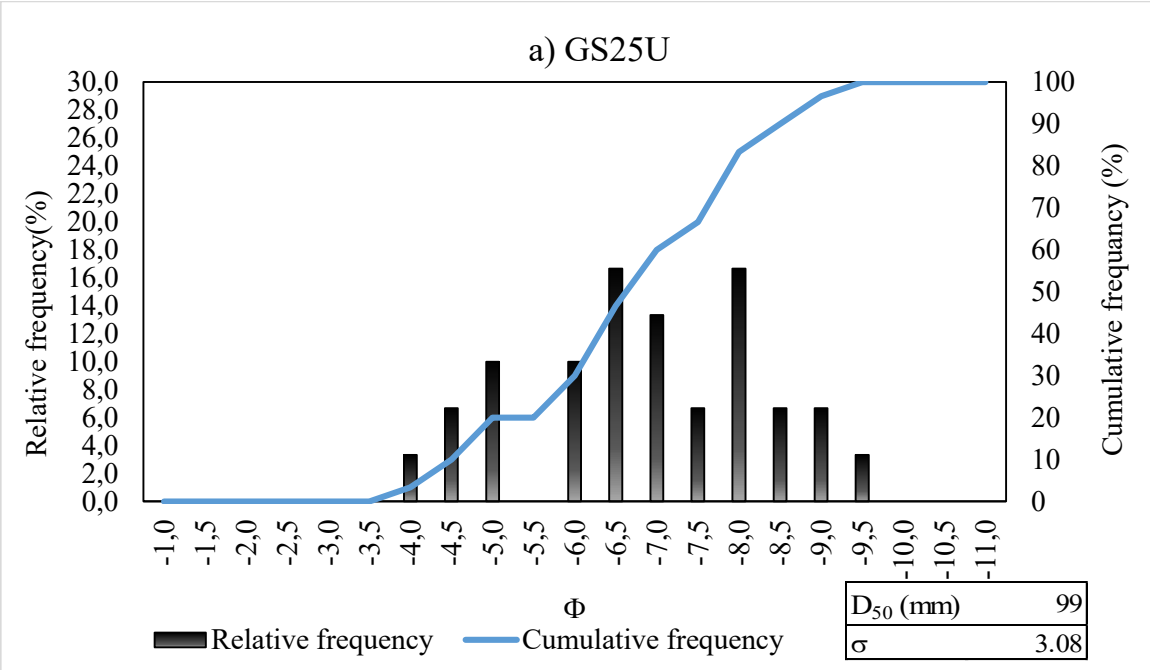

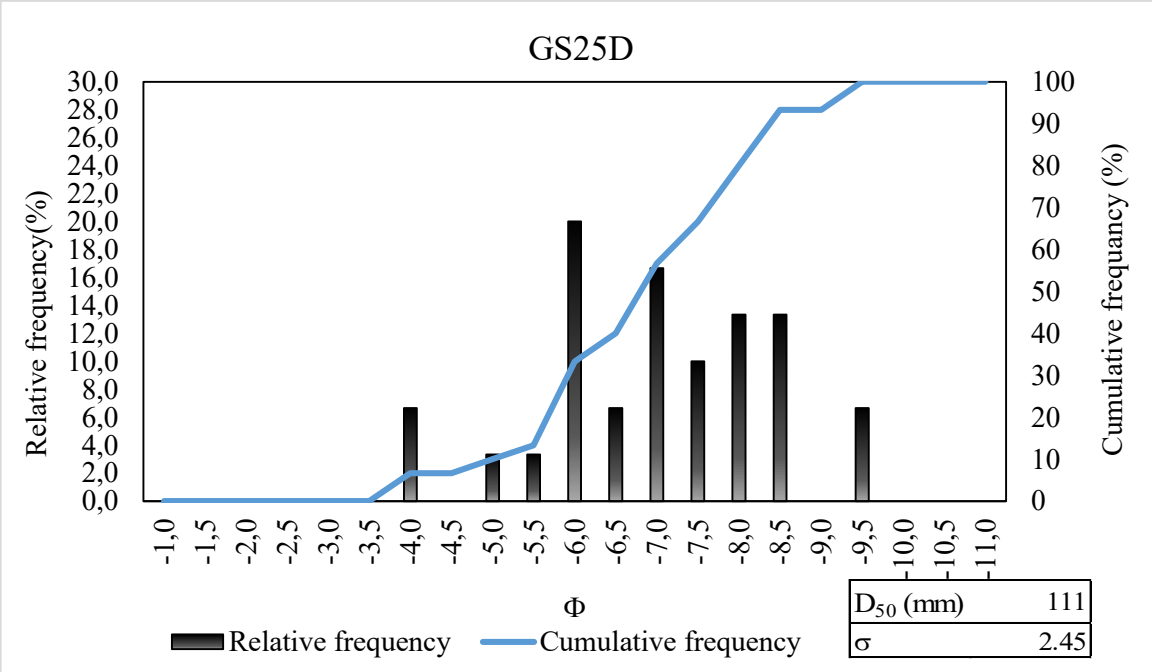
GS25D
Relative frequency(%)
Cumulative frequency (%)
Φ
Relative frequency
Cumulative frequency
D50 (mm) 111
σ 2.45

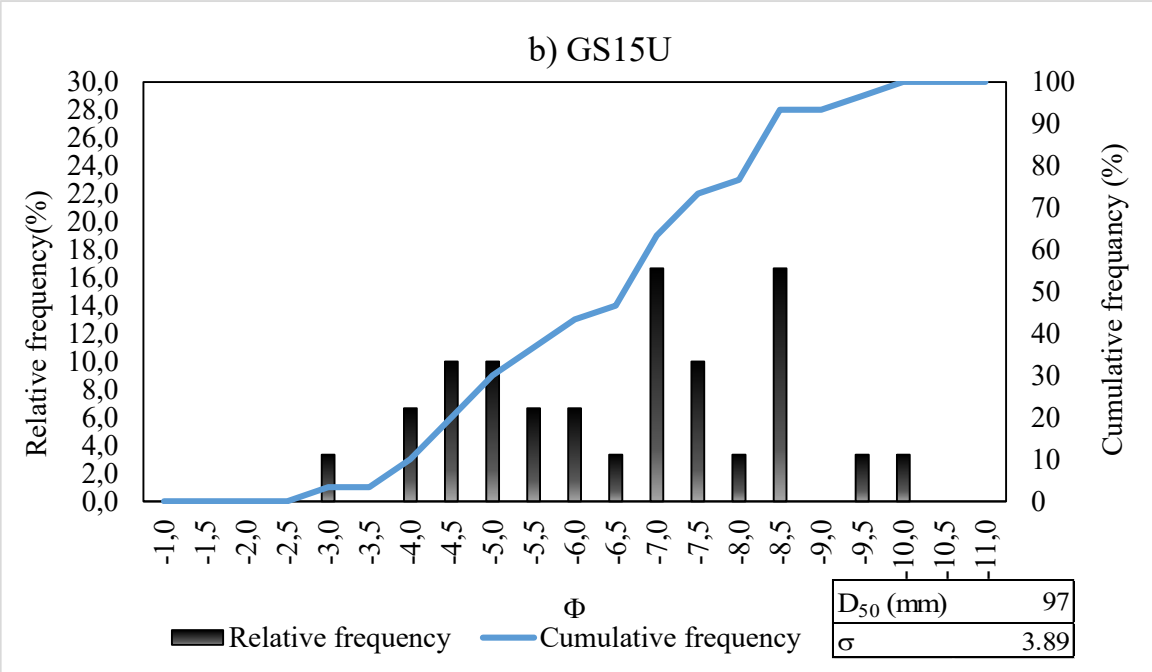
b) GS15U
Relative frequency(%)
Cumulative frequency (%)
Φ
Relative frequency
Cumulative frequency
D50 (mm) 97
σ 3.89

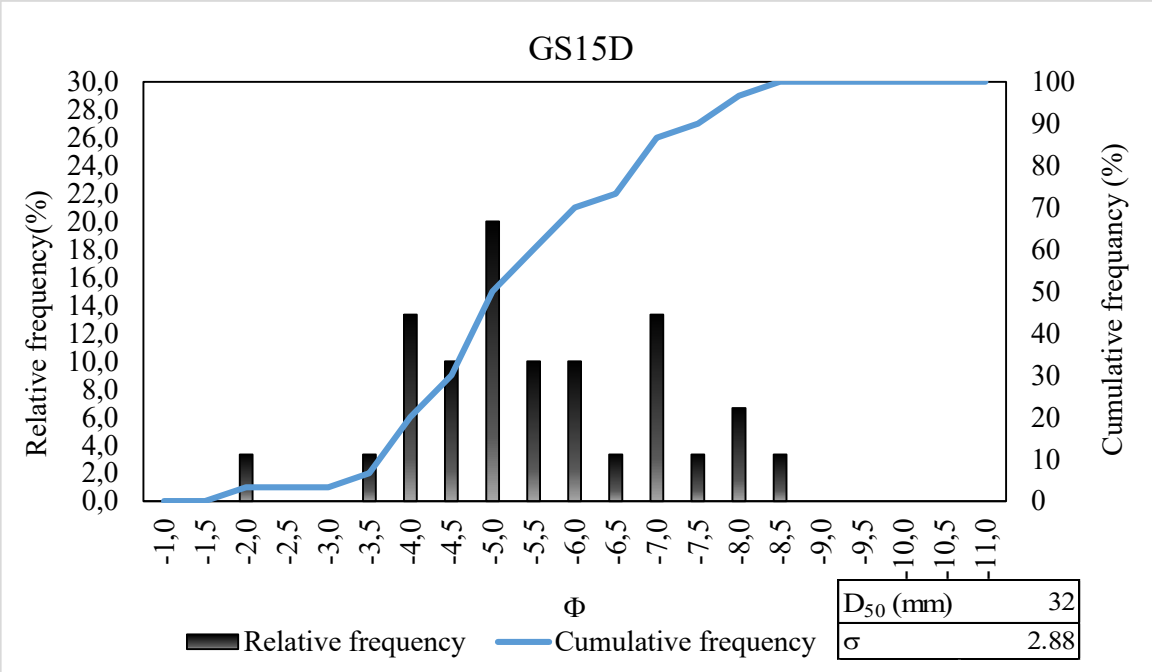
GS15D
Relative frequency(%)
Cumulative frequency (%)
Φ
Relative frequency
Cumulative frequency
D50 (mm) 32
σ 2.88

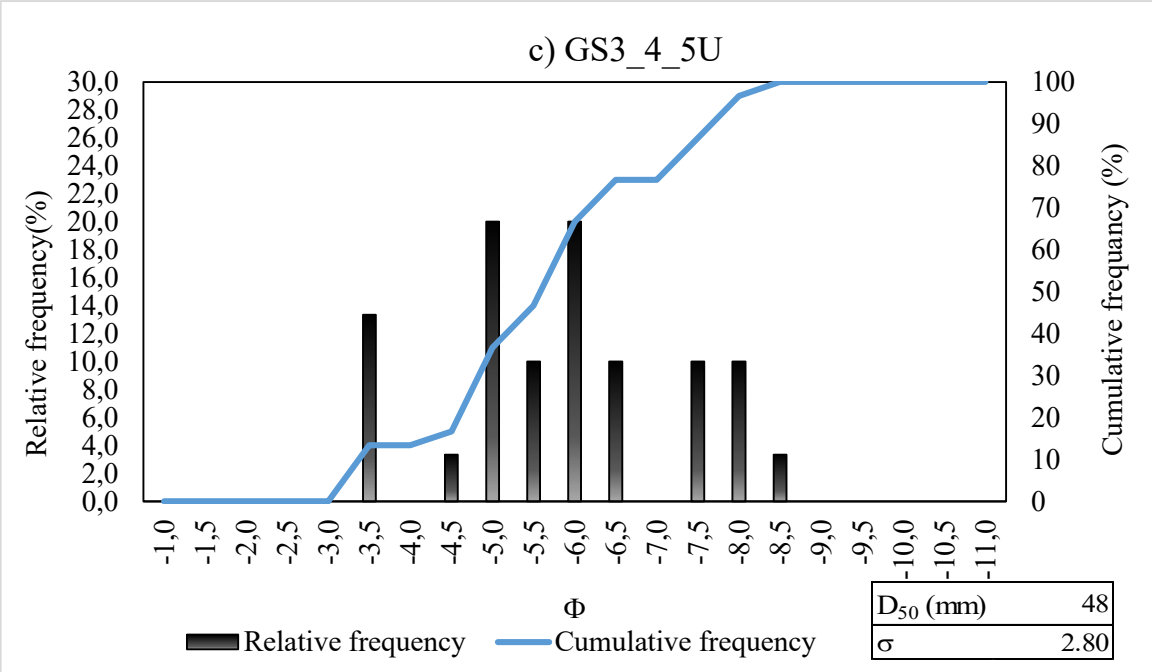
c) GS3_4_5U
Relative frequency(%)
Cumulative frequency (%)
Φ
Relative frequency
Cumulative frequency
D50 (mm) 48
σ 2.80

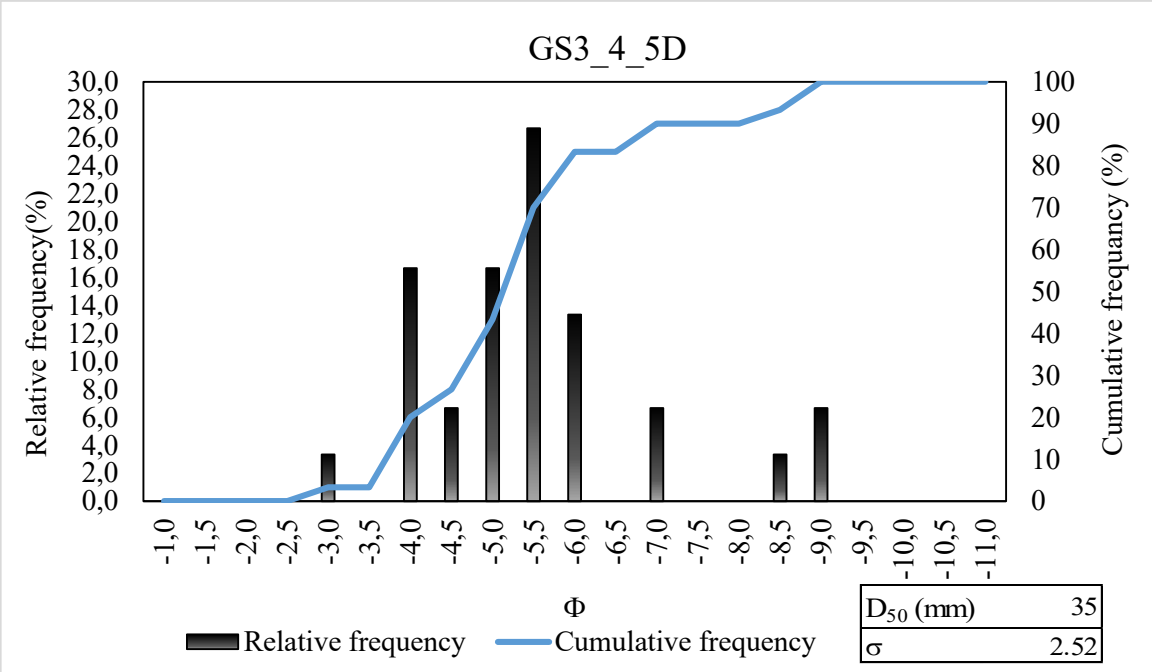

Figure 16: Grainsize distribution in the check dams a) 25 (ID F-11869-7-1); b) 15 (ID F-11869-5-1); c) 3-4-5 (ID F-11869-4-2; ID F-11869-4-3; ID F-11869-4-4) in the Vegliato Torrent.

3.3 Rainfall event

The rain event lasted only 2.5 hours (from 16:30 to 19:00 CEST) with a total precipitation of 144.2 mm. The peak precipitation is registered at 16:51 CEST, only eight minutes after the initiation of the event, with a rain depth of 4.6 mm (Fig. 17). In view of the very short duration time of the event (150 min), it is worth noticing that the majority of the precipitation is observed in the first hour, in which almost two thirds of the total rainfall (90.8 mm of 144.2 mm) is registered. The high amount of cumulated precipitation and the very short duration of the rain event indicate a return time equal or greater than 100 years. The mean intensity of the rainfall event is 57.7 mm h^{-1}. The maximum rainfall intensities, compared to the Depth-Duration Frequency for the Friuli Venezia Giulia Region, result in a return time of 2 years for I_{5min}, 10 years for I_{10min}, 15 years for I_{15min}, 50 years for I_{30min} and in a recurrence interval of more than 100 years for I_{1h}. The aforementioned characteristics of the rainfall event are summarized in Table 5.

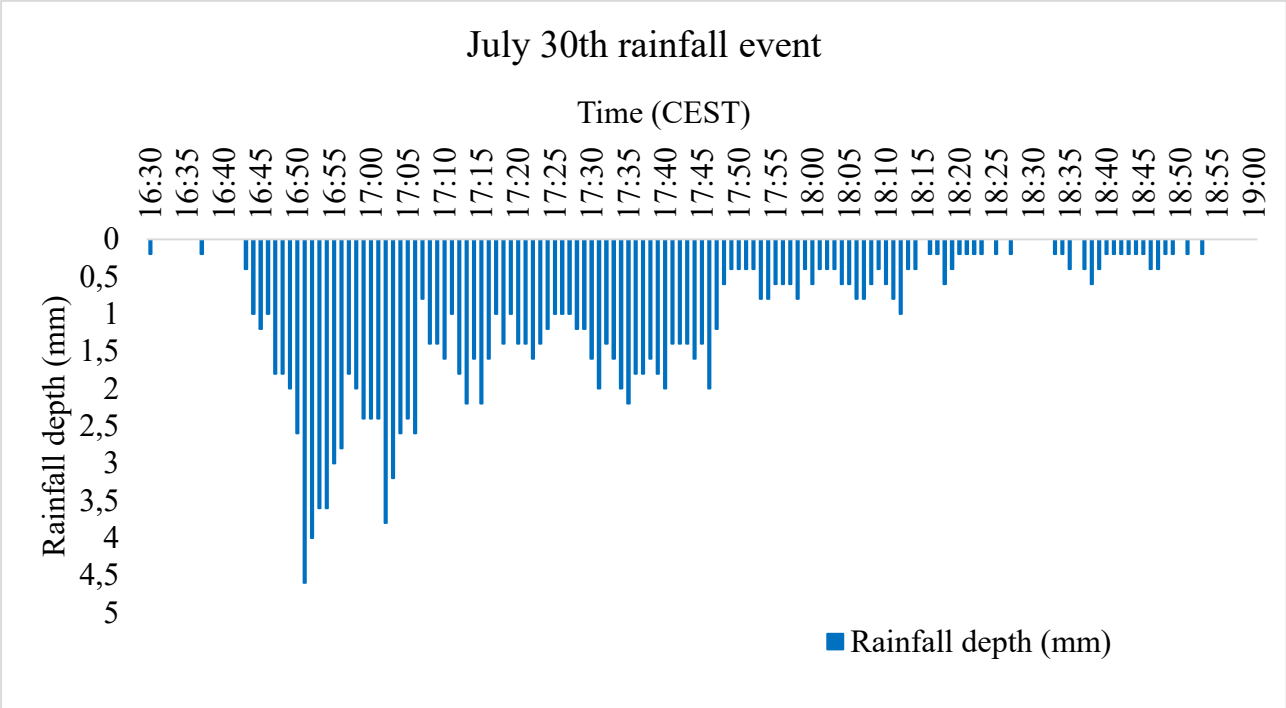

Figure 17: Rainfall depth (mm) recorded by the rain gauge of the meteorological station in Gemona del Friuli (UD) during the precipitation event in the Vegliato Torrent basin occurred on July 30th 2021 from 16:30 to 19:00 CEST.

Table 5: Main characteristics of the rainfall event. I_{5min}, I_{10min}, I_{15min}, I_{30min} and I_{1h} are the maximum rainfall intensities respectively measured for 5, 10, 15, 30 minutes and 1 hour, respectively.

Event date	7/30/2021	
Time of rainfall initiation (CEST)	16:30	
Time of rainfall end (CEST)	19:00	
Total event duration (min)	150	
Total precipitation (mm)	144.2	
Rainfall peak (mm)	4.6	
Return time (yrs)	> 100	
Mean rainfall intensity (mm h^{-1})	57.7	
Maximum rainfall intensities		Return time (yrs)
I_{5min} (mm $5min^{-1}$)	18.8	2
I_{10min} (mm $10min^{-1}$)	30.4	5
I_{15min} (mm $15min^{-1}$)	44.8	15
I_{30min} (mm $30min^{-1}$)	68.8	50
I_{1h} (mm $1h^{-1}$)	141.6	>100

3.4 Geomorphic changes

The analysis of the impacts of the 2021 flash flood on the study area reports a net widening of the active channel equal to 2.4 m. The mean bankfull width in fact increased from 29.3 m to 31.7 between pre and post-event conditions. The application of the DoD methodology for the detection and the analysis of geomorphic changes along the main channel (Fig. 18) computed a total erosion volume of 49036 ± 10898 m^3, a total deposition of 63196 ± 12877 m^3, and a consequent net deposition equal to 14160 ± 16870 m^3 (Fig. 19). The average depth of surface lowering (erosion) is 2.30 m, the average depth of surface raising (deposition) is 1.88 m and the average net thickness of difference along the 2713 m long channel is 0.26 m. On the one hand, the erosion processes are mainly localized along the banks and in two severe scours of the channel bed . On the other, the sediment deposition is distributed all along the channel but with uneven patterns. The upstream part of the main channel presents patches of high deposition, on the other hand, more spatially-distributed deposition processes with lower magnitude are present in the middle-lower section of the channel. Furthermore, the rate of detected changes in the tributaries where the check dams 9 to 14 and 27 are located is considerably lower than the differences measured in the main channel.

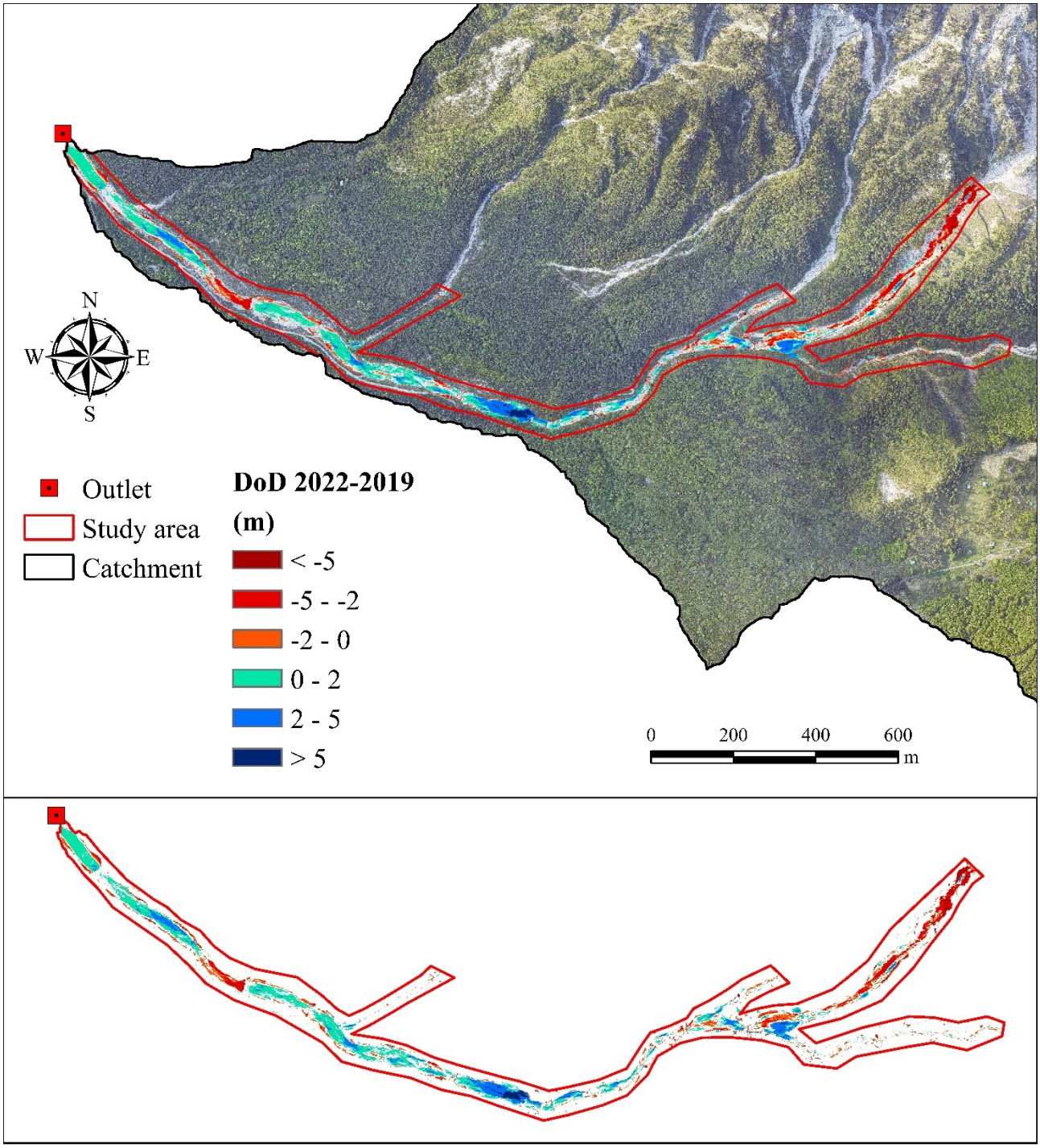

Figure 18: the response of the Vegliato Torrent main channel to the 2021 flash flood: spatial patterns of the geomorphic changes obtained through the thresholded DoD 2022 – 2019 (C.I 95%).

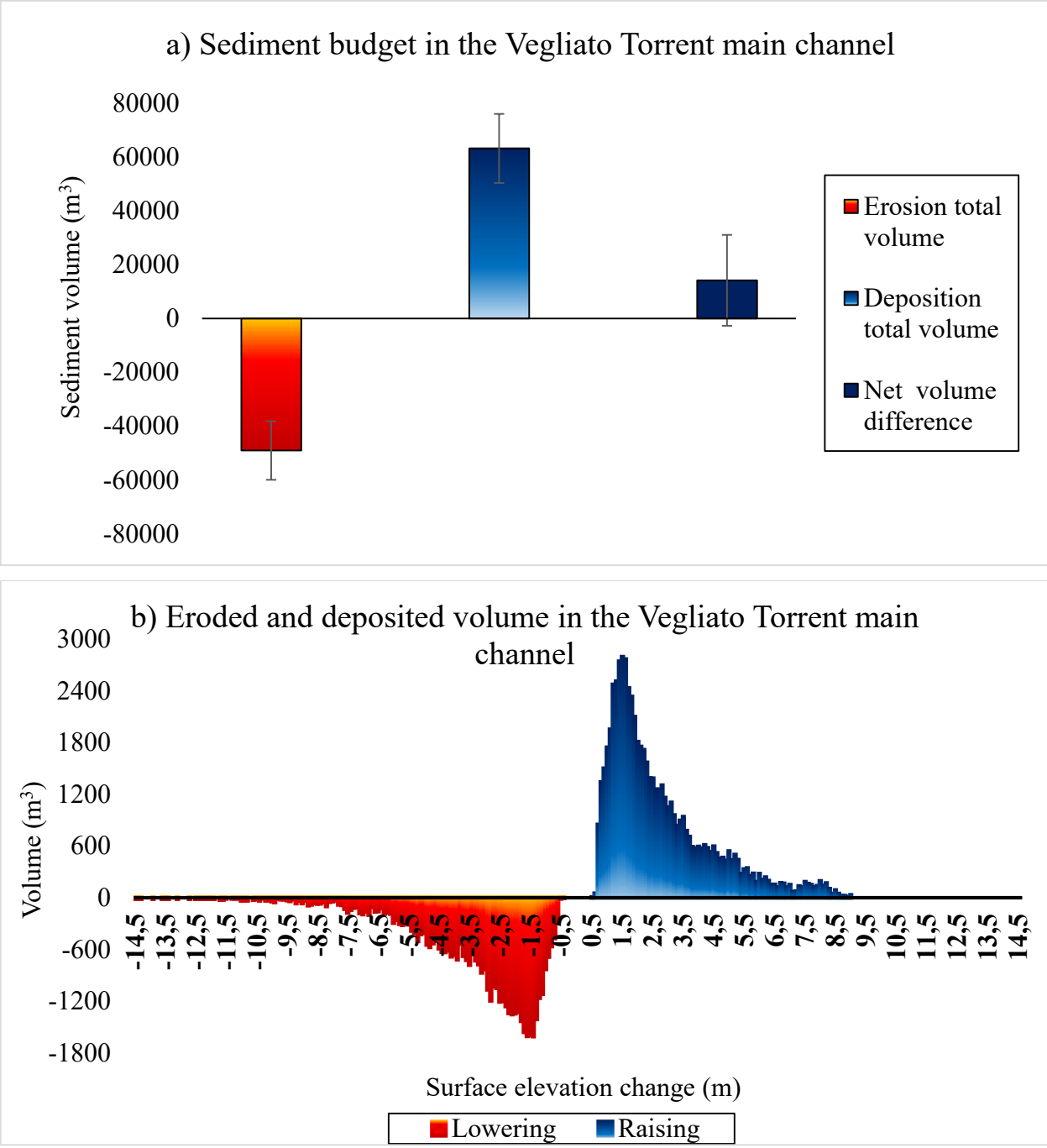

Figure 19: thresholded DoD 2022 – 2019 (C.I 95%) application in the Vegliato Torrent main channel: a) sediment budget; b) eroded and deposited volume per surface elevation change.

In Figure 20a, the deep erosional process located upstream of the check dam 28 is highlighted. This eroded part of the reach presents vertical lowering major than 5 m, including also the deepest erosion of the study area (14.5 m). In the section between the control works 23 and 28, the patterns in geomorphic change resulting from eroded banks and scour-an-fill processes in the channel bed present a strong variability. In correspondence of the outflanked check dam 25, a point of stream's diversion is present. The sediment segregation budget for the R1, comprehending the structures 23,

25, 26 and from 28 to 31, exhibits a net erosion volume equal to 19095 ± 6809 m^3. In Figure 20b, the major depositional process located between the check dams 15 and 16 is reported. This channel section presents a vertical raising mostly included between 2 and 5 m, with peaks of deposition beyond 5 m, including also the highest of the study area (9 m). In R2, in which the control works from 15 to 18 are located, the deposition processes represent the main changes even if some points of bank erosion are present, especially downstream the check dam 15. The sediment segregation budget results in a net deposited volume of 20630 ± 3379 m^3. The R3, in which the control works from 3 to 6 are located, both erosion and deposition processes are substantial (Figure 20c). Despite the large erosions, the sediment segregation budget exhibits a net deposited volume of 2778 ± 3024 m^3. The erosion processes in this reach are mainly associated to the deep excavation downstream of the check dam 6 in which 5647 ± 927 m^3 were displaced with a surface lowering between 2 and 5 m and, in some points, major that 5 m. Other considerable erosion processes in the reach are detected mainly on the banks, especially in concomitance with the sediment deposition located downstream of the check dam 3. The average vertical thickness of difference for R1, R2 and R3 are -1.11, 2.28 and 0.24 m, respectively. The sediment budget and the eroded and deposited volume per surface elevation change for the segregation areas are reported in Figure 21. The sediment budget and the change of surface depth for the main channel and for the segregation areas is reported in Table 6.

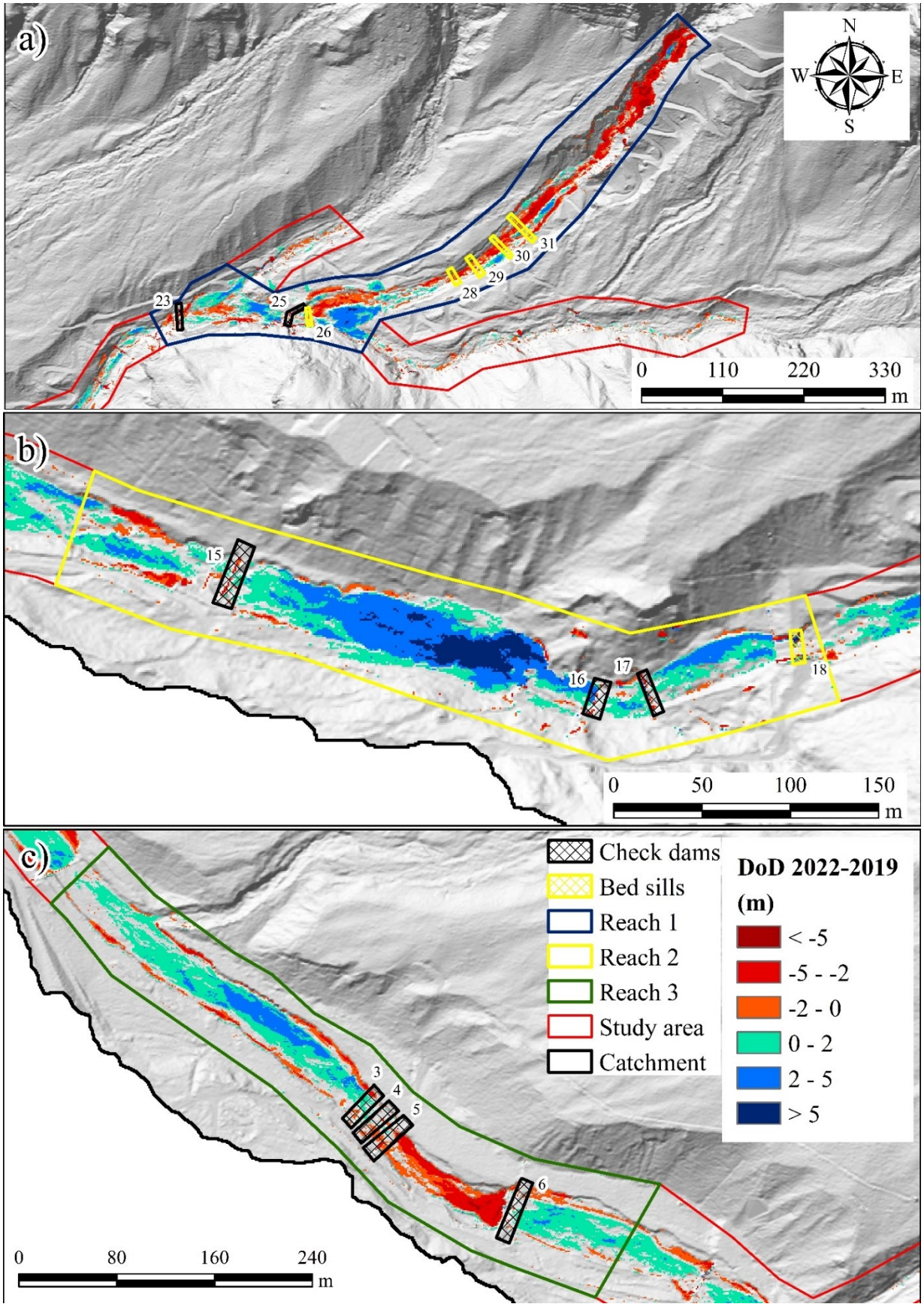

Figure 20: zoom of the geomorphic changes detected with the thresholded DoD 2022 – 2019 (C.I. 95%) in three reaches of the Vegliato Torrent and the location of the control works: a) R1; b) R2; c) R3.

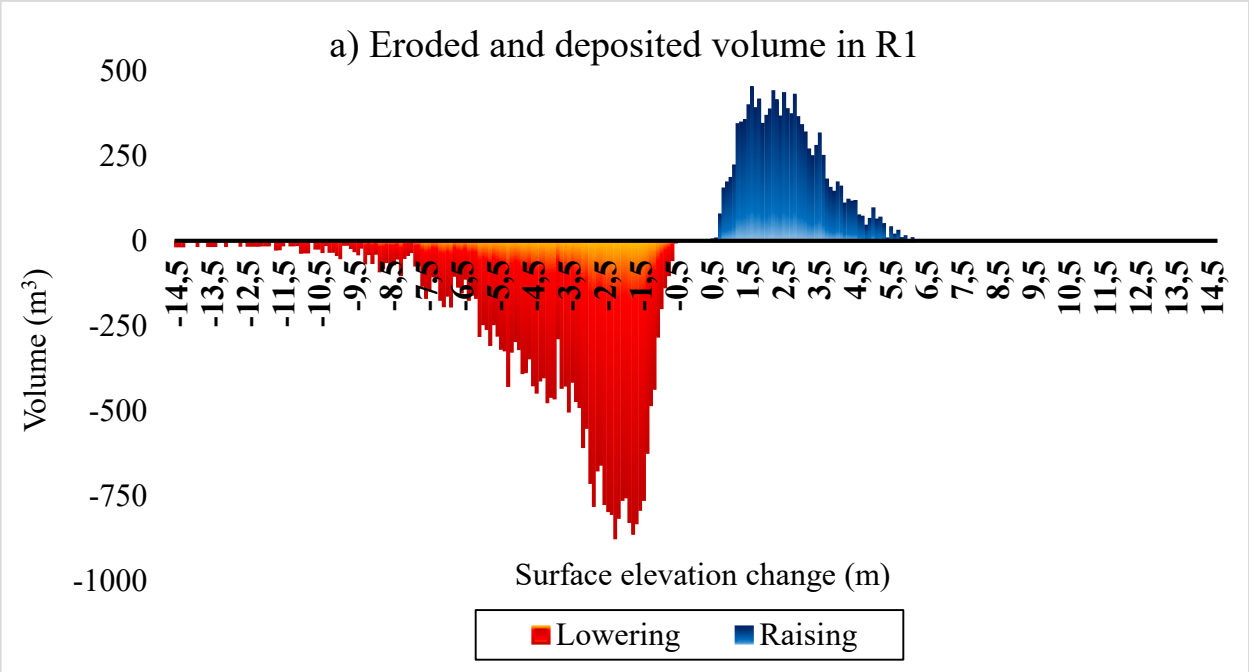
a) Eroded and deposited volume in R1
500
250
0
-250
-500
-750
-1000
Volume (m³)
-14,5
-13,5
-12,5
-11,5
-10,5
-9,5
-8,5
-7,5
-6,5
-5,5
-4,5
-3,5
-2,5
-1,5
-0,5
0,5
1,5
2,5
3,5
4,5
5,5
6,5
7,5
8,5
9,5
10,5
11,5
12,5
13,5
14,5
Surface elevation change (m)
Lowering
Raising

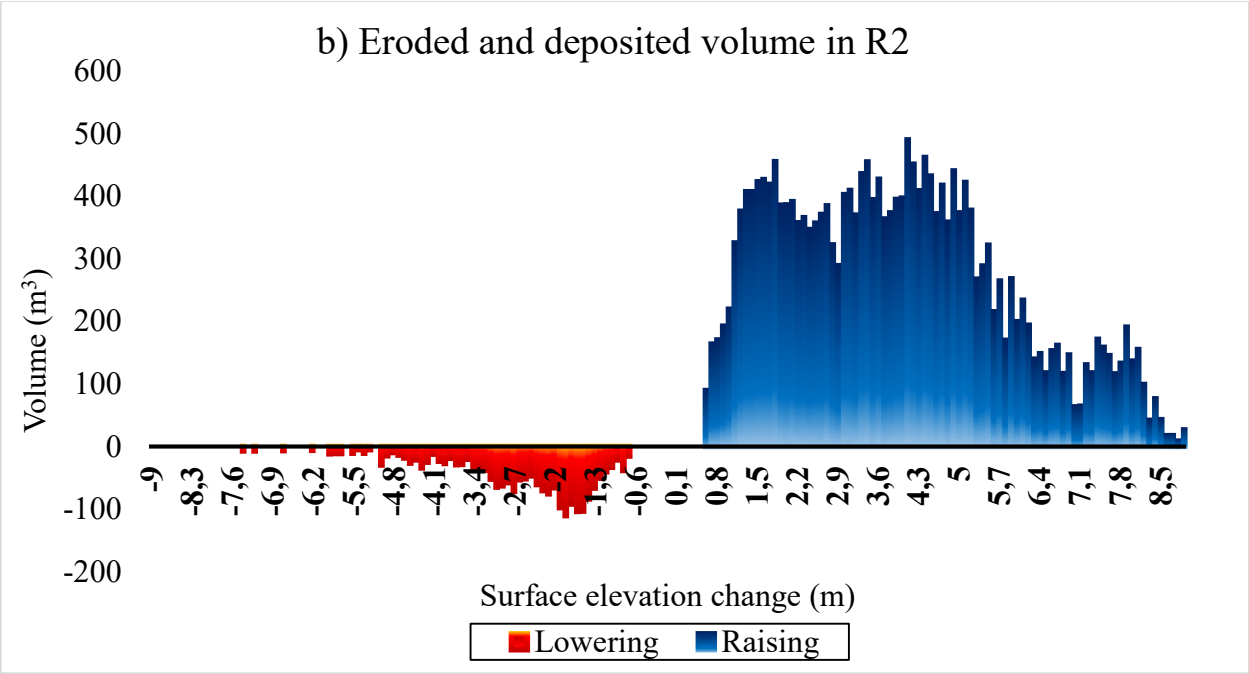
b) Eroded and deposited volume in R2
600
500
400
300
200
100
0
-100
-200
Volume (m³)
-9
-8,3
-7,6
-6,9
-6,2
-5,5
-4,8
-4,1
-3,4
-2,7
-2
-1,3
-0,6
0,1
0,8
1,5
2,2
2,9
3,6
4,3
5
5,7
6,4
7,1
7,8
8,5
Surface elevation change (m)
Lowering
Raising

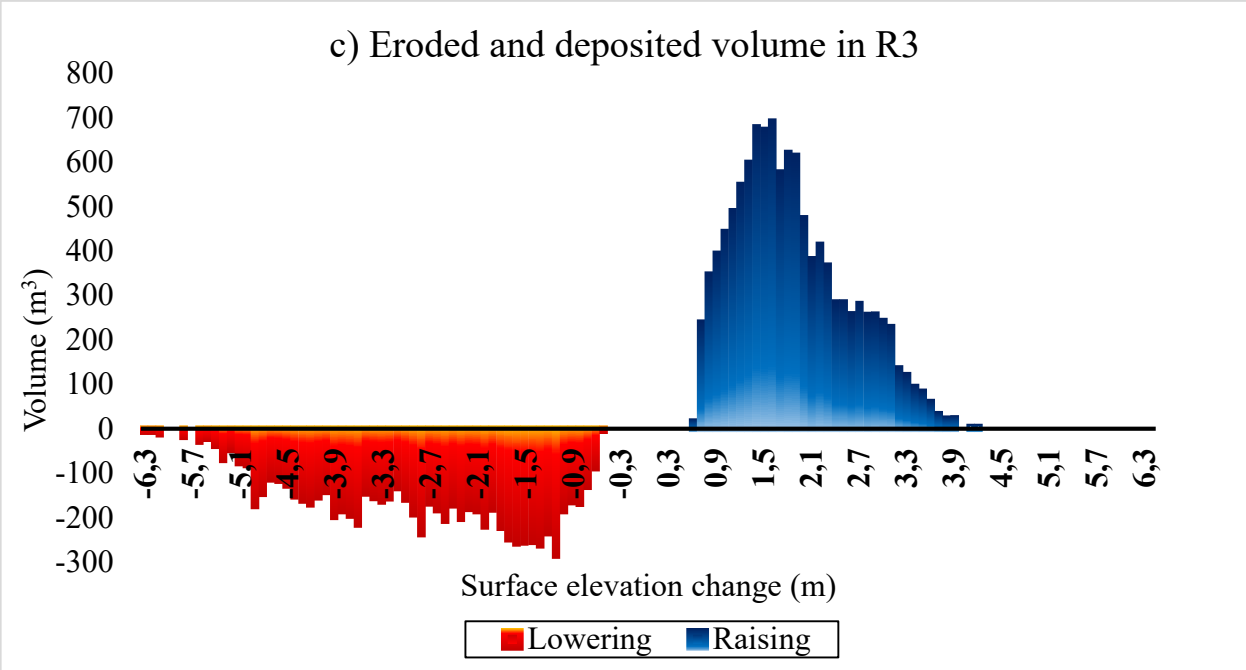

Figure 21: Eroded and deposited volume per surface elevation change resulted from the thresholded DoD 2022 – 2019 (C.I. 95%) application in the segregation areas: a) R1; b) R2; c) R3.

Table 6: Sediment budget and change of surface depth resulted from the thresholded DoD 2022 – 2019 (C.I. 95%) application in the main channel of Vegliato Torrent and in segregation areas.

		Main channel	**Segregation areas**		
			R1	**R2**	**R3**
Erosion	(m)	2.30 ± 0.51	2.70 ± 0.55	1.99 ± 0.56	2.10 ± 0.43
	(m^3)	49036 ± 10898	30784 ± 6296	2148 ± 609	8448 ± 1726
Deposition	(m)	1.88 ± 0.38	2.04 ± 0.45	2.86 ± 0.42	1.52 ± 0.34
	(m^3)	63196 ± 12877	11689 ±2591	22778 ± 3324	11227 ± 2484
Net difference	(m)	0.26 ± 0.31	-1.11 ± 0.40	2.28 ± 0.37	0.24 ± 0.26
	(m^3)	14160 ± 16870	-19095 ± 6809	20630 ± 3379	2778 ± 3024

Discussion

The 2021 flash flood occurred in the Vegliato Torrent basin deeply affected the geomorphological settings of the active channel, causing intense processes of erosion and deposition. The high-intensity rain event and its short duration, linked with the limited size of the catchment and its topographic features, generated a flash flood that reflects the characteristics of this type of events as proposed by Gaume *et al*. (2009). The topographic differences between 2019 and 2022, assessed with the application of robust DoDs, were generated mainly during the studied flash flood event, with the displacement of large quantities of sediment along the channel network. Consequently, erosion and deposition processes affecting the main channel with vertical surface variations in the order of

meters are widely present. In fact, the occurrence of important geomorphological changes in mountain streams is a well-observed phenomenon in response to high magnitude flash flood and flood events. These results are concordant with several studies analyzing flash flood- and flood-induced geomorphological changes in mountain catchments (Dean and Schmidt, 2013; Bezak *et al.* 2017; Cislaghi *et al.*, 2019; Oss Cazzador *et al.*, 2021; Pellegrini *et al.*, 2021; Rainato *et al.*, 2021).

The main erosion process localized in the upstream part of the main channel (R1) is characterized by a severe bed incision and bank erosions, which mobilized a large volume of sediment, consequently transported downstream. The displacement of such massive sediment quantity is related to a presumable rock fall that damaged the reinforced slope located upstream of the main channel, delivering a large volume of sediment and offering a easily-erodible substrate. On the other hand, this erosion process is linked to the sudden increase of surface runoff caused by the intense precipitation interplaying with the high slope degree characterizing the channel section upstream of the bed sill 28. Notably, the latter is characterized by an average slope higher than the rest of the channel (32° versus 22° of the section between control works 1 and 26). Therefore, the generation of a debris flow in this channel section is caused by the interaction of high volumes of available sediment with hydrological and gravitational forcings. These findings are in agreement with the study conducted by Cavalli *et al.* (2017), who analysed the role of topographical aspects on sediment mobilization during flood events in mountain catchments and by Cucchiaro *et al*. (2019), who studied sediment patterns of debris flow channels in the Moscardo Torrent (Eastern Alps in Friuli Venezia-Giulia region). On the contrary, the severe erosion occurred downstream of the check dam 6 (R3) is related to a different cause. The creation of a downstream scour in hydraulic structures is a widely observed issue and it is related to the power of the turbulent tumbling flow of the free fell, especially in check dams with considerable height such as the n. 6 (11 m) (Gellis *et al.*, 1995; Piton and Recking, 2017). In fact, this erosion process that resulted in the under-excavation of the check dam is not directly related to the presence of consistent sediment fluxes impacting on the hydraulic structure, rather from issues generated by an excessive height of the control work and the neglected maintenance over time. Therefore, check dam 6 is a good example of poorly maintained structure and, as indicated by Lucas-Borja *et al.* (2021), represents the negligible effects of not maintained check dams in controlling floods and the possible undesired effects that they may play in triggering erosive processes during high-magnitude flood events.

The highest variability of geomorphic changes is attested in the upper section of the channel (R1) between the check dams 23 and bed sill 28. There, the patterns of erosion and deposition tend to overlap, creating distributed patches of scoured bed accompanied by depositional ones. In this reach, the sediment pulse wandered from one bank to the other, even if in a limited spatial extent of

a hundred meters, causing the outflanking of check dam 25 with the overflow of the sediment on the adjacent forest road. In fact, the grainsize analyses and the post-event field survey of check dam 25 show how the control work behaved: i) retained sediment fluxes until its complete filling, ii) the sediment over-flooded and iii) the sediment fluxes outflanked transporting high diameter bed material downstream. This is testified by the increase of D_{50} downstream of the check dam 25 and its poor functionality (Fig. 11b). Furthermore, the variability in geomorphic processes in R1 is also reflected by the sharp increase of the sediment heterogeneity exhibited by the grainsize distribution analysis in the check dams of this section. The peculiar pattern of geomorphic processes and the different trend in grainsize distribution observed in the lower part of R1 could be related to the confluence of the main channel with the two upstream tributaries. In fact, as found by Rhoads and Kenworthy (1998) and Rhoads *et al.* (2009), stream confluences represent areas of important geomorphological changes and the characteristics of the bed material are subjected to high variability over time but, as stated by the authors, these dynamics are not widely studied and present several research gaps. Furthermore, the high heterogeneity characterizing the bed material in this section could be due to its different origin from diverse sediment source areas. However, to fully understand these processes, the analysis of the sediment source areas would be needed and, although this last represent a well-studied research field in the geomorphological community, its aims are beyond the objectives of this study.

The detection of topographic differences and their quantitative evaluation permitted to determine the spatial location and the sediment budget, i.e. the net result of deposition and erosion volumes. The sediment budget for the Vegliato Torrent main channel confirms a net aggradation of the channel network. In fact, even if erosion patterns are consistent, the deposition processes balance and overtake the displacement and recruitment of bed material along the channel. Furthermore, the deposition areas along the channel network present more defined and evenly distributed patterns and tend to be localized upstream of the check dams. In the upper section of the channel network (R1) where the Vegliato Torrent flows in the most impervious hillslopes, the channel bed exhibits a net erosion with an average vertical surface lowering of one meter, approximately. Here, the hydraulic structures were able to partially control the transported sediment volume. On the contrary, in the middle part of the channel (R2), where the topography tends to be less complex and several check dams are present, the channel bed is subjected to an average vertical surface raising of more than 2 meters. These patterns are clearly observed upstream of check dam 15, where an important depositional area almost completely balanced, in terms of sediment budget, the erosion occurred in R1. In fact, the grainsize analyses of the over-flooded check dam 15 reports a considerable effect of the control work in retaining major size bed material, efficiently sorting and retaining sediment, thus decreasing the D_{50} and the heterogeneity downstream of the check dam. On the other hand, R3

presents almost a net balance between erosion and deposition processes. In fact, even if the severe erosion downstream of the check dam 6 generated an important sediment displacement, the deposition processes were able to counterpart the scouring effect in terms of sediment budget. The sediment eroded downstream of check dam 6 deposited in a continuous *plume* without any interruption caused by check dams 3, 4 and 5 that are, indeed, assessed as not functional by any mean. These results stress again the important roles of check dams in controlling sediment fluxes. Another example is testified by the important deposition located on the bed sill 1, which was able to retain sediment limiting the possible delivery of the bed material to the outlet even if a small part of the sediment fluxes managed to trespass it. Therefore, the position of the control works in a mountain torrent is fundamental as described by Piton *et al.* (2017) and Piton and Recking (2017). Furthermore, the impacts of the control works in controlling sediment fluxes in response to a high magnitude flood are in agreement with the findings of Cucchiaro *et al.* (2019), who demonstrated the key role of check dams in controlling debris flows and in attenuating the impacts of high volume sediment fluxes.

The results presented in this thesis are obtained with the combined analysis of remote sensing data and field assessment of the control works system, which reports several hydraulic structures with ceased or compromised functionality due to sediment over-flooding and filling. Since a widely used protocol to assess the hydraulic state and functionality of structures is not present in literature, the methods for the estimation of the efficiency of the control works is based on field observations and it may result, at a certain level, biased by the subjective judgement of the operators. However, this method is able to generally estimate the efficiency of the control works system and the results can be extremely useful when combined with the quantitative estimations resulting from a robust methodology. Furthermore, the estimation of the control works net efficiency based on field surveys data is in line with the results of the DoDs. In fact, the post-event limited efficiency of the check dams assessed in the field surveys reflects the effects of the hydraulic structures on the aforementioned sediment dynamics. These findings suggest that the system of check dams and bed sills in the Vegliato Torrent played a fundamental role in the control of the 2021 flash flood. The main geomorphic processes are detected mainly in the main channel, exhibiting less activity in the three tributaries. The construction of the control works system efficiently interacted with the sediment dynamics; the structures e managed the mobilized sediment along the channel, retaining coarse sediments and boulders in the upper section (result confirmed by the grainsize distribution analysis), favoring the bed aggradation with (average slope reduction from 25.45° pre-event to 24.78° post event) and, consequently, limiting the sediment volume conveyed at the outlet.

The effects of the channel control works in controlling the sediment fluxes is traduced in the deposition of a large volume of bed material upstream of the check dams and bed sills. The time spent

in field surveys have been fundamental to evaluate the key role of the hydraulic structures in controlling sediment fluxes that are, in fact, currently over-flooded and/or filled. Therefore, in order to control future flood events, especially considering the observed global change and its effect on flood frequency and intensity, the check dams should be maintained. In fact, in their current condition, the control works can play only a limited role in controlling sediment fluxes due to their damaged or destroyed condition and to their compromised functionality, which results in a low efficiency of the whole system. The maintenance of the structures should be addresses especially on the over-flooded and filled check dams/bed sills that are not able to perform their functions and need to be emptied from the deposited sediment. In fact, the deposited bed material upstream of the control works may generate lateral over-floods if the transport capacity won't be adequate to empty the structures and, if other flash flood events occur, additional sediment may be transported by debris flows or hyperconcentrated flows. Furthermore, the check dam 6, which presents critical conditions and may be at risk of collapsing if further neglected should be taken into consideration in the maintenance. At last, if necessary, the control works system should be re-planned, considering the eventual introduction of new structures.

Conclusions

The study of the effects of the control works system on sediment dynamics in the Vegliato Torrent, affected by a flash flood in 2021, is accomplished through an integrated approach based on the detection, mapping and quantitative evaluation of geomorphic changes in the channel network. The analysis of LiDAR-derived DTMs and the application of the DoD methodology, supported by the field assessment of the control works condition and efficiency, accompanied by the analysis of the bed material texture, served to this aim. Hence, the robust methodology used to assess the flash flood-induced topographic differences is further strengthened by the analysis of the field surveys data, thus offering a detailed view of the current situation of the control works system and offering a characterization of the sediment in the channel network. The workflow adopted in this thesis to assess the fundamental role of the hydraulic structures and to estimate the post-event situation of the control works system can provide a useful tool for the development of the most appropriate strategy to maintain the existent control works, to re-establish their efficiency and/or for the planning of the installation of new ones. Furthermore, the results of this thesis can represent a starting point for future studies, focusing on the analysis not only in the channel network but on the entire catchment. In fact, the analyses of the patterns of erosion and deposition evaluated with the proposed methodology can be further improved through the assessment of the channel-hillslope connectivity and the analysis of the sediment source areas. On the other hand, the rainfall event triggering the flash flood in 2021

could be further examined by means of hydrological analyses and flood modelling to improve the prediction of the flash flood-induced effects in the study torrent.

Annex 1: database of the control works system in the Vegliato Torrent basin

N	ID	X coordinate	Y coordinate	Typology	Year	Height (m)	Width (m)	State	Functionality	Notes	Efficiency (%)
1	F-11869-3-4	356.837,376	5.128.062,508	Fordable bed sill	1980	1	51.8	Good	Compromised	Sediment over-flooded with upstream and downstream deposition	75
2	F-11869-3-6	356.926,020	5.127.941,117	Check dam	1980	1.15	54.4	Good	Operative	Functional on the right side; left side damaged	100
3	F-11869-4-2	357.166,963	5.127.740,020	Check dam	1950	1.35	31.8	Destroyed	Null	50% of the check dam presents visible foundation on the left side	0
4	F-11869-4-3	357.174,901	5.127.728,114	Check dam	1950	1.65	34.6	Destroyed	Null	10% of the check dam is still standing on the left side	0
5	F-11869-4-4	357.181,251	5.127.714,620	Check dam	1930	2.25	32.1	Destroyed	Null	20% of the check dam is still standing on the left side	0
6	F-11869-4-5	357.293,368	5.127.666,042	Check dam	1930	11	60	Damaged	Null	Check dam over-flooded by sediment; secondary check dam is pensile and downstream scoured	0
7	F-11869-4-6	357.442,453	5.127.605,550	Check dam	1980	2.3	55	Good	Null	Sediment over-flooded	0
8	F-11869-4-6_bis	357.517,594	5.127.561,099	Check dam	-	2.2	7.5	Damaged	Compromised	Wooden check dam; sediment over-flooded; not present in IRDAT (2018)	50
9	F-11874-1-1	357.562,045	5.127.580,149	Check dam	1930	3.4	16.5	Good	Compromised	Sediment over-flooded	75
10	F-11874-1-1_bis	357.585,328	5.127.590,733	Check dam	-	1.9	10.1	Destroyed	Compromised	Decayed wooden check dam damaged on the left side; sediment over-flooded; not present in IRDAT (2018)	25
11	F-11874-1-3	357.610,728	5.127.597,083	Check dam	1930	2	9	Destroyed	Compromised	Decayed wooden check dam; sediment over-flooded	25
12	F-11874-1-3_bis	357.630,836	5.127.615,075	Check dam	-	3.6	14	Good	Compromised	Not present in IRDAT (2018)	75
13	F-11874-1-5	357.652,003	5.127.630,950	Check dam	1930	1.7	9.6	Destroyed	Compromised	Wooden check dam	25
14	F-11874-1-6	357.740,903	5.127.686,777	Check dam	-	6	23.5	Good	Compromised	Not present in IRDAT (2018)	75
15	F-11869-5-1	357.791,615	5.127.436,062	Check dam	1930	9.1	34.3	Good	Null	Check dam and secondary check dam (4.25 m high); over-flooded and filled up by sediment both on the right and left side	0
16	F-11869-5-3	358.002,224	5.127.368,328	Check dam	1980	2.9	23	Good	Null	Completely sediment over-flooded	0
17	F-11869-5-4	358.032,386	5.127.373,884	Check dam	1980	3.2	34.2	Damaged	Null	Extremely sediment over-flooded; right wing damaged	0

18	F-11869-6-3	358.120,493	5.127.400,872	Bed sill	1980	-	-	Damaged	Compromised	Consistently damaged but still partially functioning	50
19	F-11869-6-4	358.197,487	5.127.422,303	Check dam	1980	2.9	27.7	Good	Null	Sediment over-flooded, filled and outflanked both on the right and left side; presence of bank defence on the left side and hillslope naturalistic engineering structure on the right side, both damaged	50
20	F-11869-6-6	358.249,742	5.127.473,369	Check dam	1980	3.8	22.5	Damaged	Compromised	-	50
21	F-11869-6-6_bis	358.261,648	5.127.497,180	Check dam	-	-	-	Destroyed	Null	Completely sediment over-flooded; not present in IRDAT (2018)	0
22	F-11869-6-7	358.274,216	5.127.519,670	Check dam	1980	4.6	24.8	Damaged	Null	Central section of the spillway over-flooded by sediment; concrete partially damaged	0
23	F-11869-6-9	358.358,883	5.127.559,358	Check dam	1980	10.5	43.1	Damaged	Null	Check dam and secondary check dam; check dam over-flooded and filled up by sediment on the right side; damaged buttress	0
24	F-11872-1-6	358.488,661	5.127.642,305	Filtering check dam	1980	2.5	25	Good	Compromised	1.7 m high filtering slot	75
25	F-11869-7-1	358.504,536	5.127.559,754	Check dam	1980	6.6	15.2	Damaged	Null	Check dam and secondary check dam (2.6 m high); check dam over-flooded and filled by sediment and outflanked on the left side with sediment on the forest road	0
26	F-11869-7-1_bis	358.531,631	5.127.563,810	Bed sill	-	-	-	Good	Null	Not present in IRDAT (2018)	0
27	F-11870-1-1	358.890,142	5.127.566,456	Check dam	1980	-	-	Good	Operative	-	100
28	F-11871-1-3	358.724,777	5.127.615,404	Bed sill	1980	1.6	16	Destroyed	Null	Bank defences in a good state both on the right and left side	0
29	F-11871-1-3_bis	358.756,527	5.127.628,633	Bed sill	-	-	-	Destroyed	Null	Sediment over-flooded and outflanked on the left side; not present in IRDAT (2018)	0
30	F-11871-1-3_tris	358.793,569	5.127.657,738	Bed sill	-	-	-	Destroyed	Null	Sediment over-flooded and outflanked both on the right and left side; not present in IRDAT (2018)	0
31	F-11871-1-3_quater	358.827,965	5.127.677,581	Bed sill	-	-	-	Destroyed	Null	Not present in IRDAT (2018)	0
											27.4

Annex 2: the median diameter and the heterogeneity of the sediment upstream and downstream of the check dams in the Vegliato Torrent.

Check dams	ID	D_{50} (mm) upstream check dam	D_{50} (mm) downstream check dam	σ upstream check dam	σ downstream check dam
2	F-11869-3-6	25	24	2.23	2.26
3 4 5	F-11869-4-2 F-11869-4-3 F-11869-4-4	48	35	2.80	2.52
6	F-11869-4-5	91	76	2.82	2.67
7	F-11869-4-6	96	37	2.96	2.51
9	F-11874-1-1	54	30	3.48	2.95
15	F-11869-5-1	97	32	3.89	2.88
16	F-11869-5-3	84	76	3.46	4.03
17	F-11869-5-4	64	70	3.07	3.45
19	F-11869-6-4	100	64	2.89	2.59
20	F-11869-6-6	64	70	3.07	3.45
22	F-11869-6-7	181	81	3.45	3.67
24	F-11872-1-6	136	91	2.83	2.56
25	F-11869-7-1	99	111	3.08	2.45
28	F-11871-1-3	114	144	2.98	2.78
		90	67	3.07	2.91

Bibliography

ArpaFVG meteo fvg. 'ARPA OSMER'. www.meteo.fvg.it. Accessed 21 October 2022. https://www.meteo.fvg.it/archivio.php.

ArpaV meteo Veneto. https://www.arpa.veneto.it/ Accessed 25 October 2022.

Baewert, Henning, and David Morche. 2014. 'Coarse Sediment Dynamics in a Proglacial Fluvial System (Fagge River, Tyrol)'. *Geomorphology*, SEDIMENT FLUX AND SEDIMENT BUDGET STUDIES IN COLD ENVIRONMENTS: NEW APPROACHES AND TECHNIQUES, 218 (August): 88–97. https://doi.org/10.1016/j.geomorph.2013.10.021.

Baker, Victor R. 1977. 'Stream-Channel Response to Floods, with Examples from Central Texas'. *GSA Bulletin* 88 (8): 1057–71. https://doi.org/10.1130/0016-7606(1977)88<1057:SRTFWE>2.0.CO;2.

Beniston, Martin. 2009. 'Trends in Joint Quantiles of Temperature and Precipitation in Europe since 1901 and Projected for 2100'. *Geophysical Research Letters* 36 (7). https://doi.org/10.1029/2008GL037119.

Bezak, Nejc, Dejan Grigillo, Tilen Urbančič, Matjaž Mikoš, Dušan Petrovič, and Simon Rusjan. 2017. 'Geomorphic Response Detection and Quantification in a Steep Forested Torrent'. *Geomorphology*, SEDIMENT DYNAMICS IN ALPINE BASINS, 291 (August): 33–44. https://doi.org/10.1016/j.geomorph.2016.06.034.

Billi, P. 1994. Morfologia dei corsi d'acqua. Verde ambiente 5, 61 – 70.

Blöschl, Günter, Julia Hall, Juraj Parajka, Rui A. P. Perdigão, Bruno Merz, Berit Arheimer, Giuseppe T. Aronica, et al. 2017. 'Changing Climate Shifts Timing of European Floods'. *Science* 357 (6351): 588–90. https://doi.org/10.1126/science.aan2506.

Borga, Marco, Markus Stoffel, Lorenzo Marchi, Francesco Marra, and Matthias Jakob. 2014. 'Hydrogeomorphic Response to Extreme Rainfall in Headwater Systems: Flash Floods and Debris Flows'. *Journal of Hydrology*, Climatic change impact on water: Overcoming data and science gaps, 518 (October): 194–205. https://doi.org/10.1016/j.jhydrol.2014.05.022.

Brasington, J., B. T. Rumsby, and R. A. McVey. 2000. 'Monitoring and modelling morphological change in a braided gravel-bed river using high resolution GPS-based survey'. *Earth Surface Processes and Landforms* 25 (9): 973–90. https://doi.org/10.1002/1096-9837(200008)25:9<973::AID-ESP111>3.0.CO;2-Y.

Brasington, James, Joe Langham, and Barbara Rumsby. 2003. 'Methodological Sensitivity of Morphometric Estimates of Coarse Fluvial Sediment Transport'. *Geomorphology* 53 (3): 299–316. https://doi.org/10.1016/S0169-555X(02)00320-3.

Bussi, G., X. Rodríguez-Lloveras, F. Francés, G. Benito, Y. Sánchez-Moya, and A. Sopeña. 2013. 'Sediment Yield Model Implementation Based on Check Dam Infill Stratigraphy in a Semiarid Mediterranean Catchment'. *Hydrology and Earth System Sciences* 17 (8): 3339–54. https://doi.org/10.5194/hess-17-3339-2013.

Cavalli, Marco, Beatrice Goldin, Francesco Comiti, Francesco Brardinoni, and Lorenzo Marchi. 2017. 'Assessment of Erosion and Deposition in Steep Mountain Basins by Differencing Sequential Digital Terrain Models'. *Geomorphology*, SEDIMENT DYNAMICS IN ALPINE BASINS, 291 (August): 4–16. https://doi.org/10.1016/j.geomorph.2016.04.009.

Cazorzi, F., dati non pubblicati, comunicazione personale

Coccolo, Alessandro, and Federico Sgobino. 1996. 'Le Colate Detritiche Quali Effetti Indiretti Del Terremoto: L'evento Del 9 giugno 1987 Nel Torrente Vegliato'. *GruppoCP* (blog). 15 November 1996. http://www.gruppocp.it/le-colate-detritiche-quali-effetti-indiretti-del-terremoto-levento-del-9-giugno-1987-nel-torrente-vegliato/.

Comiti, F., V.D. Agostino, M. Moser, M.A. Lenzi, F. Bettella, A.D. Agnese, E. Rigon, S. Gius, and B. Mazzorana. 2012. 'Preventing wood-related hazards in mountain basins: From wood load estimation to designing retention structures'. *Proceedings, 12th Congress INTERPRAEVENT 2012*, 651–62.

Cucchiaro, Sara, Federico Cazorzi, Lorenzo Marchi, Stefano Crema, Alberto Beinat, and Marco Cavalli. 2019. 'Multi-Temporal Analysis of the Role of Check Dams in a Debris-Flow Channel: Linking Structural and Functional Connectivity'. *Geomorphology* 345 (November): 106844. https://doi.org/10.1016/j.geomorph.2019.106844.

D'Agostino, V. 2013. 'Filtering-Retention Check Dam Design in Mountain Torrents'. In *Check Dams, Morphological Adjustments and Erosion Control in Torrential Streams*, 185–210.

De Marco, Jessica, Eleonora Maset, Sara Cucchiaro, Alberto Beinat, and Federico Cazorzi. 2021. 'Assessing

Repeatability and Reproducibility of Structure-from-Motion Photogrammetry for 3D Terrain Mapping of Riverbeds'. *Remote Sensing* 13 (13): 2572. https://doi.org/10.3390/rs13132572.

Devereux, Bernard, and Gabriel Amable. 2009. 'Airborne LiDAR: Instrumentation, Data Acquisition and Handling'. In *Laser Scanning for the Environmental Sciences*, 49–66. John Wiley & Sons, Ltd. https://doi.org/10.1002/9781444311952.ch4.

Doocy, Shannon, Amy Daniels, Sarah Murray, and Thomas D. Kirsch. 2013. 'The Human Impact of Floods: A Historical Review of Events 1980-2009 and Systematic Literature Review'. *PLoS Currents* 5 (April) https://doi.org/10.1371/currents.dis.f4deb457904936b07c09daa98ee8171a.

Esposito, Giuseppe, Fabio Matano, and Germana Scepi. 2018. 'Analysis of Increasing Flash Flood Frequency in the Densely Urbanized Coastline of the Campi Flegrei Volcanic Area, Italy'. *Frontiers in Earth Science* 6. https://www.frontiersin.org/articles/10.3389/feart.2018.00063.

Gaume, Eric, Valerie Bain, Pietro Bernardara, Olivier Newinger, Mihai Barbuc, Allen Bateman, Lotta Blaškovičová, et al. 2009. 'A Compilation of Data on European Flash Floods'. *Journal of Hydrology* 367 (1): 70–78. https://doi.org/10.1016/j.jhydrol.2008.12.028.

Gellis, Allen C., Andres Cheama, Vanissa Laahty, and Sheldon Lalio. 1995. 'Assessment of Gully-Control Structures in the Rio Nutria Watershed, Zuni Reservation, New Mexico1'. *JAWRA Journal of the American Water Resources Association* 31 (4): 633–46. https://doi.org/10.1111/j.1752-1688.1995.tb03390.x.

Giorgi, F., Eun-Soon Im, Erika Coppola, Noah Diffenbaugh, Xin-jing Gao, Laura Mariotti, and Y Shi. 2011. 'Higher Hydroclimatic Intensity with Global Warming'. *Journal of Climate* 24 (October): 5309–24. https://doi.org/10.1175/2011JCLI3979.1.

Heritage, George, and David Hetherington. 2007. 'Towards a Protocol for Laser Scanning in Fluvial Geomophology'. *Earth Surface Processes and Landforms* 32 (January): 66–74. https://doi.org/10.1002/esp.1375.

IRDAT, http://irdat.regione.fvg.it/WebGIS/, 2018

James, L. Allan, Michael E. Hodgson, Subhajit Ghoshal, and Mary Megison Latiolais. 2012. 'Geomorphic Change Detection Using Historic Maps and DEM Differencing: The Temporal Dimension of Geospatial Analysis'. *Geomorphology*, Geospatial Technologies and Geomorphological Mapping Proceedings of the 41st Annual Binghamton Geomorphology Symposium, 137 (1): 181–98. https://doi.org/10.1016/j.geomorph.2010.10.039.

Lague, Dimitri, and Baptiste Feldmann. 2020. 'Topo-Bathymetric Airborne LiDAR for Fluvial-Geomorphology Analysis'. In *Remote Sensing of Geomorphology*, edited by Simon M. Mudd (Eds.) Paolo Tarolli, 23:25–54. Developments in Earth Surface Processes. Elsevier. https://doi.org/10.1016/B978-0-444-64177-9.00002-3.

Lane, Stuart, Richard Westaway, and Murray Hicks. 2003. 'Estimation of Erosion and Deposition Volumes in a Large, Gravel-Bed, Braided River Using Synoptic Remote Sensing'. *Earth Surface Processes and Landforms* 28 (March): 249–71. https://doi.org/10.1002/esp.483.

Lucas-Borja, Manuel Esteban, Guillaume Piton, Yang Yu, Carlos Castillo, and Demetrio Antonio Zema. 2021. 'Check Dams Worldwide: Objectives, Functions, Effectiveness and Undesired Effects'. *CATENA* 204 (September): 105390. https://doi.org/10.1016/j.catena.2021.105390.

Lucía, Ana, Marc Schwientek, Joachim Eberle, and Christiane Zarfl. 2018. 'Planform Changes and Large Wood Dynamics in Two Torrents during a Severe Flash Flood in Braunsbach, Germany 2016'. *Science of The Total Environment* 640–641 (November): 315–26. https://doi.org/10.1016/j.scitotenv.2018.05.186.

Marchi, Lorenzo, Marco Borga, Emanuele Preciso, and Eric Gaume. 2010. 'Characterisation of Selected Extreme Flash Floods in Europe and Implications for Flood Risk Management'. *Journal of Hydrology* 394 (November): 118–33. https://doi.org/10.1016/j.jhydrol.2010.07.017.

Marchi, Lorenzo, Francesco Comiti, Stefano Crema, and Marco Cavalli. 2019. 'Channel Control Works and Sediment Connectivity in the European Alps'. *Science of The Total Environment* 668 (June): 389–99. https://doi.org/10.1016/j.scitotenv.2019.02.416.

Pellegrini, Giacomo, Lorenzo Martini, Marco Cavalli, Riccardo Rainato, Antonio Cazorzi, and Lorenzo Picco. 2021. 'The Morphological Response of the Tegnas Alpine Catchment (Northeast Italy) to a Large Infrequent Disturbance'. *Science of The Total Environment* 770 (May): 145209. https://doi.org/10.1016/j.scitotenv.2021.145209.

Piton, Guillaume, Simon Carladous, Alain Recking, Jean Marc Tacnet, Frédéric Liébault, Damien Kuss, Yann Quefféléan, and Olivier Marco. 2017. 'Why Do We Build Check Dams in Alpine Streams? An

Historical Perspective from the French Experience'. *Earth Surface Processes and Landforms* 42 (1): 91–108. https://doi.org/10.1002/esp.3967.

Piton, Guillaume, and Alain Recking. 2017. 'Effects of Check Dams on Bed-Load Transport and Steep-Slope Stream Morphodynamics'. *Geomorphology*, SEDIMENT DYNAMICS IN ALPINE BASINS, 291 (August): 94–105. https://doi.org/10.1016/j.geomorph.2016.03.001.

Podobnikar, Tomaž, Dr Zoran Stancic, and Krištof Oštir. n.d. 'DATA INTEGRATION FOR THE DTM PRODUCTION', 7.

Rainato, R., L. Martini, G. Pellegrini, and L. Picco. 2021. 'Hydrological, Geomorphic and Sedimentological Responses of an Alpine Basin to a Severe Weather Event (Vaia Storm)'. *CATENA* 207 (December): 105600. https://doi.org/10.1016/j.catena.2021.105600.

Rodriguez-Lloveras, Xavier, Gianbattista Bussi, Félix Francés, Emilio Rodriguez-Caballero, Albert Solé-Benet, Mikel Calle, and Gerardo Benito. 2015. 'Patterns of Runoff and Sediment Production in Response to Land-Use Changes in an Ungauged Mediterranean Catchment'. *Journal of Hydrology* 531 (December): 1054–66. https://doi.org/10.1016/j.jhydrol.2015.11.014.

Romero-Díaz, A., P. Marín-Sanleandro, and R. Ortiz-Silla. 2012. 'Loss of Soil Fertility Estimated from Sediment Trapped in Check Dams. South-Eastern Spain'. *CATENA* 99 (December): 42–53. https://doi.org/10.1016/j.catena.2012.07.006.

Shakti, P.C., Tsuyoshi Nakatani, and Ryohei Misumi. 2018. 'Hydrological Simulation of Small River Basins in Northern Kyushu, Japan, During the Extreme Rainfall Event of July 5–6, 2017'. *Journal of Disaster Research* 13 (2): 396–409. https://doi.org/10.20965/jdr.2018.p0396.

Tarolli, Paolo. 2014. 'High-Resolution Topography for Understanding Earth Surface Processes: Opportunities and Challenges'. *Geomorphology* 216 (July): 295–312. https://doi.org/10.1016/j.geomorph.2014.03.008.

Turowski, Jens M., Elowyn M. Yager, Alexandre Badoux, Dieter Rickenmann, and Peter Molnar. 2009. 'The Impact of Exceptional Events on Erosion, Bedload Transport and Channel Stability in a Step-Pool Channel'. *Earth Surface Processes and Landforms* 34 (12): 1661–73. https://doi.org/10.1002/esp.1855.

Victoriano, Ane, James Brasington, Marta Guinau, Gloria Furdada, Mariló Cabré, and Myriam Moysset. 2018. 'Geomorphic Impact and Assessment of Flexible Barriers Using Multi-Temporal LiDAR Data: The Portainé Mountain Catchment (Pyrenees)'. *Engineering Geology* 237 (April): 168–80. https://doi.org/10.1016/j.enggeo.2018.02.016.

Wang, Yafeng, Liding Chen, Bojie Fu, and Yihe Lü. 2014. 'Check Dam Sediments: An Important Indicator of the Effects of Environmental Changes on Soil Erosion in the Loess Plateau in China'. *Environmental Monitoring and Assessment* 186 (7): 4275–87. https://doi.org/10.1007/s10661-014-3697-6.

Wechsler, Suzanne. 2003. 'Perceptions of Digital Elevation Model Uncertainty by DEM Users'. *URISA Journal* 15 (January): 57–64.

Wechsler, Suzanne P., and Charles N. Kroll. 2006. 'Quantifying DEM Uncertainty and Its Effect on Topographic Parameters'. *Photogrammetric Engineering & Remote Sensing* 72 (9): 1081–90. https://doi.org/10.14358/PERS.72.9.1081.

Wheaton, Joseph, James Brasington, Stephen Darby, and David Sear. 2009. 'Accounting for Uncertainty in DEMs from Repeat Topographic Surveys: Improved Sediment Budgets'. *Earth Surface Processes and Landforms* 35 (December): 136–56. https://doi.org/10.1002/esp.1886.

Wheaton, Joseph M. 2008. 'Uncertainty in Morphological Sediment Budgeting of Rivers', 434.

Wheaton, Joseph M., James Brasington, Stephen E. Darby, Alan Kasprak, David Sear, and Damiá Vericat. 2013. 'Morphodynamic Signatures of Braiding Mechanisms as Expressed through Change in Sediment Storage in a Gravel-Bed River'. *Journal of Geophysical Research: Earth Surface* 118 (2): 759–79. https://doi.org/10.1002/jgrf.20060.

Wilhelm, B., F. Arnaud, D. Enters, F. Allignol, A. Legaz, O. Magand, S. Revillon, C. Giguet-Covex, and E. Malet. 2012. 'Does Global Warming Favour the Occurrence of Extreme Floods in European Alps? First Evidences from a NW Alps Proglacial Lake Sediment Record'. *Climatic Change* 113 (3): 563–81. https://doi.org/10.1007/s10584-011-0376-2.

Zanferrari, A., Masetti, D., Monegato, G., Poli, M., E., Avigliano, R., Carraro, F., Faranda, C., Grandesso, P., Ligios, P., Podda, F., Ponton, M., Rigo, M., Roghi, M., Romano, R., Russo, S., Stefani, C. 2011. 'Note illustrative della carta geologica d'Italia alla scala 1:50.000, foglio 049, Gemona del Friuli'. Istituto Superiore per la Protezione e la Ricerca Ambientale (ISPRA), Servizio Geologico d'Italia